Hindawi
Journal of Chemistry
Volume 2022, Article ID 7062912, 19 pages
https://doi.org/10.1155/2022/7062912

Review Article

Manganese Schiff Base Complexes, Crystallographic Studies, Anticancer Activities, and Molecular Docking

Ayodele Temidayo Odularu

School of Further and Continuing Education, Faculty of Education, University of Fort Hare, Private Bag X1314, Alice 5700, South Africa

Correspondence should be addressed to Ayodele Temidayo Odularu; 201106223@ufh.ac.za

Received 23 November 2021; Revised 14 June 2022; Accepted 16 June 2022; Published 24 August 2022

Academic Editor: Maria C. Yebra-Biurrun

Choice of ligands is significant to successful synthesis of metal complexes (coordination compounds). This study reports the use of Schiff base as the right ligand to control the poor bioavailability and neurodegenerative toxicity challenges of manganese ion. In line with this study, document analysis was used as the methodological approach to evaluate the significance of Schiff base ligands in easing these manganese's challenges and aligning the resultant coordination compounds (manganese Schiff base complexes) as therapeutic agents in anticancer studies. Report also involves crystallographic studies where single crystal X-ray crystallography was used as a chemical characterization technique. In addition, molecular docking studies, MOE2008, and AutoDock software were used to reveal the mode of interaction between the Schiff base and the manganese(II) and (III) ions, as well as scrutinizing the biological efficacy of the manganese(II) and manganese(III) Schiff bases coordination compounds as anticancer agents against some anticancer cell lines. Conclusion drawn was that manganese(II) and manganese(III) Schiff bases coordination compounds gave more active and potent activities than the corresponding Schiff bases. As a result, challenges of neurodegenerative toxicity and poor bioavailability of manganese ion were overcome, and the chelation therapy was fulfilled. Results from single crystal X-ray crystallography confirmed the successful synthesis of manganese(II) and manganese(III) Schiff bases coordination compounds and revealed the mechanism of reaction, while the molecular docking buttressed the biological activities of the Schiff base ligand and manganese Schiff base coordination compounds by portraying the structure activity relationship (SAR) between either Schiff base or the manganese Schiff base coordination compounds and the virtual cancer cell line (receptor protein), where hits were obtained for lead optimizations.

1. Introduction

According to Sangram Singh, "maintaining a good health should be everyone's main focus" [1]. In agreement with Sangram Singh quote, medicinal inorganic chemists are contributing to overcome the challenges of using conventional carbon-based anticancer drugs, such as dosage toxicity, insolubility, multiple drug resistance (MDR), neurogenerative toxicity, and poor bioavailability being faced in the health sector [2, 3]. One important way medicinal inorganic chemists helped to overcome these challenges is the use of metal-based compounds, although the use of metals had been in use since human history.

Metal-based compounds have upper edges over conventional carbon-based anticancer drugs because of the capability of ligands in a three-dimensional configuration to ligate with metals, therefore permitting groups "functionalization, which can be designed for distinct molecular targets [2, 4]. In addition, these metal-based compounds also provide a prosperous environment to construct upon them different distinct molecular structures with a wide spectrum of coordination numbers and geometries, as well as kinetic effects which cannot be realized with conventional carbon-based compounds [2, 5]. Metal's oxidation state is also an essential consideration in metal-based compounds (coordination compounds)" design, which enables them to contribute significant roles in optimal

doses and bioavailabilities of the administered agents to biological chemistry [2, 6, 7].

In the case of the transition metals, the partially filled "d orbitals" they possess help them to express their interesting redox chemistry via electronic properties and their abilities to act as suitable probes in anticancer agents' designs [2, 5]. Additionally, the ability to go through ligand exchange reactions provides numerous opportunities for ligands to interact and coordinate with metals (ligate), to form metal complexes (coordination compounds), such as cisplatin [2, 8, 9]. Since the serendipitous breakthrough discovery of cisplatin's biological activity, metal-based compounds have proffered opportunities for therapeutic designs to study and treat varieties of human ailments [2, 7, 10–14]. Till date, cisplatin is still one of the most active anticancer metal-based drugs of clinical relevance. However, because of the challenges of anticancer drug resistance and side effects, such as discomfort, pain, and vomiting experienced in the use of cisplatin, other novel metal-based anticancer complexes were developed and others are in the process of development [15, 16].

Awatade et al. recounted that, for targeted treatment for anticancer drug resistance, the application of two or more drugs is better to overcome these challenges. In line with this, the synthesis of metallodrugs involving Schiff bases and their transition metal complexes is fundamental in various syntheses and medicinal chemistry [17]. Recently, numerous anticancer studies were dedicated to copper(CuII/III), iron(FeII/III), osmium(OsII/III), ruthenium(RuII/III), vanadium(VIII/IV/V), and manganese(II/III/IV). The studies revealed their bioinorganic complexes to induce reactive oxygen species (ROS) and human cancer cell death [18–22]. The most significant transition metals used in controlling numerous severe human diseases are iron and copper [23].

However, the rationale for the study of manganese coordination compounds as anticancer agents was first due to its physicochemical features clearly resembling those of iron which made manganese an important micronutrient for most creatures in the environment. Second, among all metals, manganese (Mn) is a needed cofactor for many prevalent enzymes (biological catalysts) [24–28]. Third, it is the second most abundant transition metal on the Earth's surface, indicating accessibility [29]. Fourthly, its various oxidation states are from −3 to +7, where +2, +3, and +4 are the most widespread in nature, more widely studied, and more human health complied (compliant) [2, 3, 29].

Fifthly, according to the table in Sarma et al.'s study on the biological applications of manganese Schiff base complexes, statistics showed four references for manganese's antimicrobial studies, four references for manganese's antioxidation studies, and only two references for manganese's anticancer (cytotoxic) studies, which indicated limited studies on anticancer studies of manganese complexes [20]. Sixthly, according to Table 1 in Sarma et al.'s study on the biological applications of manganese(II/III) Schiff base complexes, statistics showed five references for manganese's antimicrobial studies, four references for manganese's antioxidation studies, forty-seven references for manganese's catalytic studies, and only two references for manganese's anticancer (cytotoxic) studies, which indicated another limited study on anticancer studies of manganese complexes [21].

Neil and Zheng stated that, with manganese's physicochemical features, such as clearly resembling those of iron, its enzyme cofactor nature, its abundancy, its variable oxidation states, and its limited studies, human evidence confirms that distinct factors such as age, ethnicity, gender, genetics, and previous health conditions could aggravate manganese toxicities [30]. Neil and Zheng and Zhang et al. reported the challenges of unattached ionic manganese as "poor bioavailability and neurodegenerative toxicity" [30, 31]. They suggested suitable ligands forming stable chelation with manganese as solution in overcoming these challenges. In support of Zhang et al., Flora et al. and Pal et al. stated that ideal medical treatment to reduce metals' toxic effects is chelation therapy [32, 33].

According to Pal et al., chelation therapy is a specific therapy used for removing heavy elements from the human body by formation of a chelate complex with right chelating ligands, such that the complex has less affinity for essential metal, has less side effects, is easily removed from the body system, and is water-soluble and very stable [33]. Heavy metals belong to the class of metallic/metalloids elements with a higher density when compared with water [33]. Numerous reported sources of environmental heavy metals include agriculture, atmosphere, geology, industries, and pharmaceuticals. Most of the heavy metal ions are naturally carcinogenic, resulting in severe health distresses for both animal and plants. Some essential heavy metals, such as Co, Cr, Cu, Fe, Mg, Mo, Mn, Ni, and Zn, are nutrients needed for numerous biochemical and physiological functions, which are mainly for growth of life systems in both plants and animals [33].

However, these heavy metals produce adverse effects on the biological systems when they exceed their optimum levels' ranges, resulting in various deficiency diseases. They also damage several organs like blood circulation, brain, kidney, liver, and nerve transmission [33]. Similar to Pal et al.'s properties for right chelating ligands, Flora et al. suggested six features of ideal chelators as follows: better affinity to compete with natural chelators, capability to enter cell membranes, speedy removal of the toxic metal, extraordinary water solubility, ability to form nontoxic coordination compounds, and equivalent distribution as the metal [32].

In another study, Martin et al. stated that significant public health challenges are neurodegenerative diseases, such as Alzheimer's disease, amyotrophic lateral sclerosis (ALS), Parkinson's disease (PD), and prion disease. Additionally, these diseases could be due to high concentrations of heavy metals, such as manganese (Mn), which might enhance their negative developments [34]. Martin et al. suggested chelation therapy as a prospective therapeutic and evolving treatment for Mn overload [34]. Additionally, there are bioinformatics' methods to ascertain novel potential targets and therapeutic drugs to reverse the neurodegenerative diseases [34]. Bioinformatics analysis is used to

Table 1: Results of cytotoxic activities of metal complexes, standard bleomycin, and garlic acid.

Samples		90% confidence limit (ppm)			
	c	Lower	Upper	Regression equation	X^2
$[Mn(Fcd)(COO)_2]$	8.14	5.02	13.19	$Y = 3.7959 + 3.224x$	0.3776
$[Co(Fcd)(COO)_2]$	12.38	8.06	19.02	$Y = 3.650 + 1.2353x$	0.1290
$[No(Fcd)(COO)_2]$	19.52	12.72	30.13	$Y = 3.542 + 1.052x$	0.1650
$[Cu(Fcd)(COO)_2]$	17.95	11.50	28.00	$Y = 3.644 + 1.081x$	0.0955
$[Zn(Fcd)(COO)_2]$	36.03	22.71	57.16	$Y = 3.142\_1.19x$	0.1992
Standard bleomycin	0.41	0.276	0.620	$Y = 3.16 + 2.00x$	0.62
Garlic acid	4.53	3.330	6.150	$Y = 3.93 + 1.62x$	1.25

ascertain key genes and pathways, via predicting possible molecular mechanisms underlying Mn-induced neurotoxicity and neurodegeneration. In other words, bioinformatics analysis is important to identify new targets for manganese treatment [34].

In view of the fact that chelation therapy eases manganese challenges, crystallographic studies were used to observe the mechanism of coordination of the Schiff base to the manganese(II) and (III) ions, while molecular docking studies were reported first to identify the orientation, as well as conformation of the ligand with the receptor, and second to study the potential interaction between the Schiff base ligand or manganese Schiff base complexes and the active sites of virtual cancer cell line such as the 3HB5 receptor to obtain lead optimization [35].

The aim of this research was to explore how Schiff base ligand was used to overcome challenges of manganese's poor bioavailability and neurogenerative toxicity via coordination with manganese ion to fulfill the chelation therapy. Additionally, this study also explored the mechanism of Schiff base coordination to manganese ions via crystallography, as well as manganese Schiff base complexes' therapeutic impacts in overcoming cancer disease via anticancer studies with biological assays, and simulated (computer-generated) mode of interaction between the Schiff base ligand, synthesized manganese Schiff base coordination compounds, and cancer cell lines via molecular docking.

2. Cancer

After cardiovascular disease, the most common cause of global death is cancer. According to the prediction of the World Health Organization (WHO), there will be seventy percent rise in the number of new cases of cancer disease worldwide over the next sixteen years; therefore, it is a global disease [36]. This high cancer mortality is alarming despite several therapeutic advances, such as chemotherapy, gene profile, radiation, and surgery. As a result, direct compound manipulation that controls apoptosis, that is, a programmed cell death process, is a motivating approach to treat cancer.

According to Al-anbaky et al., approximately one-third of women in the Western world were diagnosed with human breast cancer which causes extensive mortality and develops metastases [37]. In line with the causes, it has been observed that limitations, such as general targeting, increased drug resistance, and toxicity to normal tissues, demerit many breast cancer therapies. Additionally, with the use of conventional therapy, a forty percent recurrence rate was reported for advanced breast cancer, after the diagnosis and removal of the primary tumor. In other words, these cancer cells escape cell death process and were resistant to cytotoxic drugs' treatment. As a result, new therapeutic approaches are needed to induce cancerous cell death by apoptosis or inactivate cancer cells without damaging normal cells.

3. Manganese

Manganese (Mn) is the twelfth element in the periodic table, the second most abundant element on the Earth, and the fifth transition metal in the series of first row transition metals [30]. Manganese is an essential trace element and transition metal required for several physiological processes. Milatovic and Gupta defined manganese (Mn) as an essential element to maintain appropriate functions and structures of numerous biochemical and cellular reactions [38]. Sarma et al. defined manganese as a transition metal which has affinity to bond with different types of ligands such as porphyrin (natural Schiff base) to form manganese Schiff base complexes [20]. These synthesized corresponding manganese Schiff base complexes with mixed manganese Schiff ligand complexes are applied for therapeutic purposes.

Manganese plays a significant role in the biochemistry and physiology in numerous living organisms and has a fundamental function as cofactor of numerous enzymes required for glial and neuronal cells [34, 39, 40]. However, despite its developmental and reproductive impacts on animals and humans, manganese is regarded as an environmental contaminant, because it has toxic impacts on animals and humans. The toxicity of manganese is principally linked with neurological effects and its extreme accumulation in special brain areas, such as the globus pallidus, striatum, and substantia nigra, to produce neurotoxicity, resulting in a degenerative brain disorder. Additionally, the Mn overload has demerits of neurodegenerativeness, neurotoxicity, and disease development. Chelation therapy has been applied to treat symptoms associated with Mn overexposure. However, some restrictions such as deficient specificity of chelating molecules, difficulty to cross the blood-brain barrier, and prospective common and severe adverse impacts in patients receiving chelation therapy obstruct effective treatment.

3.1. Chelation Therapy and Manganese's +2, +3, and +4 Oxidation States. The human compliant Mn's oxidation states are +2, +3, and +4. The divalent oxidation state of

manganese (Mn^{2+}) is the most stable among other oxidation states (+2, +3, and +4). In terms of geometry, the most common geometry of Mn^{2+} is octahedral; nevertheless, tetrahedral and square geometries also occur. Mn(II) freely oxidizes in alkaline solution to Mn(III) or Mn(IV) and has no ligand field stabilization energy in the high-spin state. However, in the low-spin electron configuration, it has 20 Dq units of crystal field stabilization energy. In Mn(III), d forms limited compounds contrary to Mn(II) and fairly stable in either an ionic or neutral coordination compounds with commonest geometry in the high-spin state as distorted octahedral due to Jahn Teller distortion.

According to Al-anbaky et al., manganese is a redox active metal which could affect the cellular redox homeostasis to produce reactive oxygen species (ROS) to destroy cancer cells [37]. However, at times, the manganese's concentration in the millimolar (mM) range used to destroy cancer cells might be quite high (in mM range), and very limited studies are available on biomedical applications of Mn(III) complex. Mn(IV) is most stable in anionic complexes and is subjected to hydrolysis and reduction. Nevertheless, when certain polydentate ligands such as Schiff bases coordinate with manganese, these tendencies may not always be followed.

4. Ligands

Ligands can modify biological activities by controlling the adverse effects of excess metal ion and simplifying metal-ion distributions [41, 42]. Some of the numerous studied manganese coordination compounds comprise ligands, such as chrysin, hydrazine, thiosemicarbazone, and Schiff base. The general structural formula of Schiff base is shown in Figure 1 [4].

Among several ligands, this study recognizes Schiff base because, as reported by Kajal et al., it is a versatile pharmacophore used for drug design, improving numerous bioactive lead compounds, with less side effects [43]. Nine areas of its versatile pharmacophore are analgesic, anticancer, anticonvulsant, antidepressant, antiglycation, anthelmintic, antimicrobial, antioxidant, and antitubercular applications [43]. Schiff base could be regarded as having a bioactive core, which has aroused researchers' interests to apply it as a medicinal agent [44].

4.1. Schiff Base. In 1864, Hugo Schiff discovered Schiff base [45]. A Schiff base is structurally recognized as azomethine or imine group [46–48]. The azomethine group (C=N) enables Schiff base to be active and functional [43]. Schiff base formation entails reaction of either an aliphatic or aromatic amine with an aldehyde or ketone under certain conditions [49]. The general formula for Schiff base is $R^1R^2C = NR^3$ (R^1R^2 and R^3 are either alkyl, aryl, cycloalkyl, or heterocyclic group) [45]. All the Schiff bases introduced and used previously till this contemporary era are synthetic Schiff bases. The only natural Schiff base is corrin, which has several C=N groups [45]. Corrin is a heterocyclic compound, whose name reflects the core of vitamin B_{12} (cobalamins)

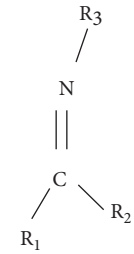

Figure 1: General structural formula of Schiff base.

[50]. Corrin ring resembles the porphyrin ring in haemoglobin [51]. Both rings have four pyrrole-like subunits structured in a ring with large conjugated alternating double and single bonds [52]. The difference between corrin's ring structure and that of porphyrin is the deficient of one of the carbon rings which connects the pyrrole-link units into a fully conjugated structure.

Another closely related biological structure, which is an intermediary between corrin and porphyrin, is chlorin [52]. Chlorin is tetrapyrrole pigment which is partly hydrogenated porphyrins [52]. It is found in chlorophyll, has conjugated bonds with only six of the eight edge carbons functional, and possesses twenty carbon atoms like the porphyrins [52, 53]. As a result, chlorin derived its name from chlorophyll. Chlorophyll is magnesium-containing chlorin, which occurs as photosynthetic pigment in chloroplasts [54]. Additionally, corroles are corrins' aromatic derivatives [55]. Schiff bases have wide industrial uses and biological applications, such as antidiabetic, anti-inflammatory, and antimalarial activities [43, 56–63].

5. Transition Metal Complexes (Coordination Compounds) as Anticancer Agents

Research shows the significant progress in the application of transition metal complexes, such as Au(I/III), Cu(II), Fe(II/III)), Mn(II/III/IV), Pt(II/IV), Ru(II/III), and Ti(IV) complexes, as drugs to treat various human diseases [64–67]. They are more distinct than nontransition metallic compounds due to their transition metals possessing unpaired electrons from partially filled d electrons and their variable oxidation states, which are involved in various biological processes [29, 64–68]. These processes are electron transfer, catalysis, and structural functions, which are often associated with active sites of enzymes and proteins [69–72].

Four decades ago, several transition metal coordination compounds possessing certain anticancer active molecules with biological potentials were assessed and screened for their anticancer *in vitro* and *in vivo* activities, while others are at different stages of clinical studies [73]. Among all these metal complexes, manganese complexes are significant with the perspective of their applications in biology, pharmaceutical chemistry, and as catalysts in organic syntheses, biological applications, and pharmaceutical chemistry [20]. Nevertheless, during normal biochemical processing, some essential metals, such as manganese, freely involve themselves in the development of various pathological disorders, such as cancer [23, 74].

5.1. Manganese(II), Mn(III), and Mn(IV) Complexes. In opposition to Neil and Zheng and Zhang et al.'s posits that manganese ion has poor bioavailability and neurodegenerative toxicity, Chang stated that manganese complexes were essential in the field of bioinorganic chemistry and their inhibitory effects as antiproliferation of the some cancer cells have been tested to yield exciting experimental results which were very exciting because they showed extraordinary anticancer activities [75]. Haque et al. stated that dissolved manganese is an important biological ion, while Prihantono et al. regarded manganese as a nontoxic metal [76, 77]. However, synergistic effects are usually observed when ligands coordinate with manganese ions to form manganese coordination compounds with reduced level of toxicity applicable for anticancer studies. The reduced level of toxicity makes Chang et al.'s, Haque et al.'s, and Prihantono et al.'s conclusions very similar to the posits by Neil and Zheng, Zhang et al., Floral et al., and Pal et al. [30, 31, 75–77].

6. Manganese(II) and Manganese(III) Schiff Base Complexes and Their Crystallographic Activities

After syntheses of Mn(II) and Mn(III) Schiff base coordination compounds, characterization techniques, such as crystallography, are used to confirm successful coordination of the Schiff base ligand to Mn(II) and Mn(III) ions. In line with crystallography, this study reports six different crystallographic activities from five different researchers.

6.1. Chang et al.'s Crystallographic Activity. Chang et al. collected the X-ray data for three samples of Mn(II) complexes on a Bruker Smart-1000 CCD diffractometer (λ 0.71073 Å, graphite-monochromated Mo-Kα radiation) at 298(2) K [75]. The structures for three samples of Mn(III) complexes were refined with full-matrix least-square methods, while the nonhydrogen atoms on F2 were refined with anisotropic thermal parameters using SHELX-97 program. All hydrogens were placed at perfect positions, while subsequent and eventual data were corrected using SADABS method [75].

6.2. Damercheli et al.'s Crystallographic Activity. Damercheli et al. collected the diffraction data for four manganese(III) Schiff base complexes at room temperature with a Bruker APEX II CCD area-detector diffractometer using Mo-Kα radiation ($\lambda = 0.71073$ Å) at 298(2) K [78]. Further processes entailing unit cell determination, cell refinements, data reductions, and absorption corrections were performed using multiscan methods with Bruker software. The structures were solved by direct methods using SIR2004, nonhydrogen atoms were refined anisotropically by the full-matrix least-squares method on F2 using SHELXL, and all hydrogens were placed at calculated positions and constrained via riding model on their parent atoms [78].

6.3. Qian et al.'s Crystallographic Activity. Qian et al. collected X-ray (intensity) data for the Mn(II) complex on a Bruker Apex II CCD diffractometer using graphite-monochromated Mo-Kα radiation ($\lambda = 0.71073$ Å) at 298(2) K [79]. For data processing and absorption correction, the packages SAINT and SADABS were used. Similar to Chang et al. and Damercheli et al., Qian et al. solved the structure of the Mn(II) complex with direct methods and refined it with full-matrix least-squares based on F2 using SHELXL-97 [75, 78, 79]. The nonhydrogen atoms were refined anisotropically, while the hydrogen atoms in the hydrated Mn(II) complex were located from different in Fourier maps, while the residual hydrogen atoms were fixed with thermal parameters and placed at geometrical positions [79].

6.4. Seck et al.'s Crystallographic Activity. Seck et al. grew Mn(II) complex crystals suitable for X-diffraction in methanol by slow evaporation. Diffraction data collection was carried out on an Enraf-Nonius Kappa-CCD diffractometer with graphite-monochromatized Mo-Kα radiation ($\lambda = 0.71073$ Å) at 293 K [80]. Contrary to Chang et al. and Qian et al., Seck et al. corrected data was for Lorentz and polarization effects but did not apply any absorption correction [75, 79, 80]. Similar to Damercheli et al., Chang et al., Qian et al., and Seck et al. solved the structure by direct methods to reveal the positions of all nonhydrogen atoms, and the Mn(II) complex scattering factors were taken from the SHELXTL program package [75, 78–80]. The structure was anisotropically refined on F2 by a full-matrix least-squares procedure for all nonhydrogen atoms. The hydrogen atoms and NH groups of the hydrated Mn(II) complex were located from different Fourier maps and refined, while other H atoms (CH and CH_3 groups) were geometrically optimized and refined as riding model by AFIX instructions [80].

6.5. Bermejo et al.'s Crystallographic Activity. Bermejo et al. obtained single crystals of Mn(III) complex by slow evaporation process of the methanolic solution at room temperature [81]. Similar to Chang et al. and Qian et al., Bermejo et al. carried out the measurements on a Bruker-SmartCCD-1000 diffractometer using graphite-monochromated Mo-Kα radiation ($\lambda = 0.71073^{\circ}$A) but at a temperature of 100 K [75, 79, 81]. The structure was also solved by direct method and refined by full-matrix least-square method based on F2. The SADABS was used as the empirical absorption correction and all hydrogen atoms were involved in the model at geometrically calculated positions [81].

6.6. Keypour et al.'s Crystallographic Activity. Similar to Bermejo et al., Keypour et al. grew dark brown single crystals from the vapor diffusion of diethyl ether into methanol [81, 82]. Contrary to the Mo-Kα radiation used by Chang et al., Qian et al., and Bermejo et al., Keypour et al. collected data for the Mn(III) complex on a XtaLAB Synergy diffractometer with mirror monochromated Cu-Kα radiation ($\lambda = 1.54184$ Å) at 100 K [62, 79, 81, 82]. Olex2 was used to

solve and refine the structure with the SHELXT structure solution program with Intrinsic Phasing and SHELXL refinement package using least-squares minimization on F2, respectively. Contrary to the SADABS used by Chang et al., Qian et al., and Bermejo et al., Keypour et al. applied Gaussian absorption corrections to the data [62, 79, 81, 82]. Anisotropic displacement parameters were used to refine the nonhydrogen atoms, while all hydrogen atoms were placed at geometrical estimates and refined using the riding model.

Concisely, five researchers among the six researchers on crystallographic studies used graphite-monochromated Mo-Kα radiation ($\lambda = 0.71073^{\circ}$A), while Keypour et al. were the only group of researchers who used mirror-monochromated Cu-Kα radiation ($\lambda = 1.54184$ Å) [75, 78–82].

7. Assays, Their Methods, and Materials for Anticancer Studies

Sequentially after successful synthesis and relevant chemical characterization techniques confirmed synthesized compounds, the biological application via the use of assay is done. This biological assay is usually used to examine and assess the anticancer potentials and potencies of synthesized compounds (samples) on tested cancer cell lines [80]. The in vitro cell culture study is a common method to screen anticancer compounds for their drug potencies and to understand their anticancer activities in an in vitro environment [75]. According to Li, *in vitro* cell culture studies are useful tools to screen chemotherapeutic agents and they give introductory data for further related studies [22]. The two assays usually used for anticancer studies compounds in in vitro environment are 3-(4,5-dimethylthiazol-2-yl)-2,5-diphenyltetrazolium bromide (MTT) and sulforhodamine B (SRB) assays. However, anticancer activities entailing the MTT assay have more studies carried out using it than the SRB assay. Five groups of researchers specified using MTT assay to determine cell viability [22, 24, 37, 78, 83].

7.1. 3-(4,5-Dimethylthiazol-2-yl)-2,5-Diphenyltetrazolium Bromide Assay (MTT). Li et al. carried out cytotoxicity studies on four Mn(II) complexes to evaluate (screen) them for their cell viabilities with MTT essays [22]. As a result, cell lines of HL-M60 were grown in RPMI-1640 medium, A549 were grown on Ca-co2 medium, and HeLa were grown in RPMI-DMEM medium at a temperature of 37°C, with 5% CO_2 and 95% air in the CO_2 incubator for 24 h. Various concentrations of the synthesized Mn(II) complexes were added to the cell culture and the incubation continued for another 48 h. Subsequently, the MTT was dissolved in the three incubated media and further incubated for 4 h. The purple formazan crystals were solubilized with the addition of 100 mL of DMSO. The absorbance was measured at 570 nm with ELISA reader, and the values are the average mean from at least triplicate independent experiments, which were measured at the percentage ratio of the absorbance of the treated cells to the untreated controls. The IC_{50} results were determined by percentage plot of the cell inhibition against concentration by the nonlinear regression analysis [22]. Ahmed et al. defined IC_{50} values as the concentrations of the Schiff base ligand (L) and its metal complexes needed to produce 50% cell growth inhibition [58]. The mean IC_{50} is the material concentration that reduces cell growth by 50% under the experimental conditions and is the average of triplicate measurements that were reproducible and statistically significant. The IC_{50} is defined as the concentration of an inhibitor where the response is reduced by half testing viability via an MTT assay [84]. In other words, the dose of cytotoxic compound where 50% viability is achieved is the IC_{50} when testing viability through an MTT assay [84, 85].

Li did the MTT assay to evaluate cell viability and cell selectivity [24]. Hence, A549 cancer cells were plated at a density of approximately 4×10^3 viable cells per well in 96-well plate. Cells were pretreated with 10 μmolL^{-1} DFO (deferoxamine) and 100 μmol L^{-1} ferric citrate. Subsequently, complex for 24, 36, and 48 h and various concentrations (3–15 μmol L^{-1}) of LMnAc were used to treat cells in quintuplicate. After incubation for the indicated time, the MTT assay was performed to measure cell viability using a 96-well plate reader [24]. Li explored the selectivity of LMnAc against the liver cancer cells (Hep-G2) and the nonmalignant liver epithelial cells (WRL-68) [24].

According to Al-anbaky et al., the MTT assay is a microculture tetrazolium assay and a colorimetric method to measure cell viability as an indicator of cytotoxicity and to assess the toxic effects of the compound [37]. The principle of MTT assay is based on the evidence that the yellow water-soluble substrate 3-(4,5-dimethylthiazol-2-yl)-2,5-diphenyltetrazolium bromide is reduced into an insoluble coloured formazan product by mitochondrial succinate dehydrogenase enzyme in blood cells [37]. The activity level relates to the viability of the cells, since the reduced MTT could only occur in metabolically active cells. The percentage (%) of cell viability was evaluated using the following equation [37]:

$$\text{Cell inhibition} = \left(\frac{\text{absorbance value of test compound} - \text{absorbance value of blank}}{\text{absorbance value of control} - \text{absorbance value of blank}} \right) \times 100. \quad (1)$$

According to Damecheri et al., MTT-based cell proliferation assay was used to determine cytotoxicity of the synthesized complexes and to evaluate growth inhibition [78]. The cancer cells were incubated with various concentrations of the complexes (0–80 μM) in a 96-well microplate for 24 h using unlabeled cells as control. Stock solutions of the complexes were prepared by dissolving the manganese(II) complexes in 1 mL of DMSO and diluted in

RPMI medium, followed by addition of 100 μL of each complex to the wells to obtain a final concentration ranging between 0 and 80 μM, and the absorbance was measured at 570 nm using a multiplate reader. After incubation for the indicated intervals, 20 μL of an MTT solution in phosphate buffer saline (PBS; 2 mg mL^{-1}) was added to each well and the plates were wrapped in aluminium foil and incubated at 37°C for 2 h. Each concentration was tested in triplicate to avoid experimental error. Survival percentage was calculated as a negative control fraction. The half-maximal inhibitory concentration (IC_{50}) values for the inhibition of cell growth were obtained from the dose-response curve with Pharm software [78], while with the usual cancer cell lines they acted against human breast (MCF-7) and human liver adenocarcinoma (Hep-G2) cancer cells. The purpose of the cytotoxicity assay is to determine if the metal complexes are significantly active against both types of cell lines at the preclinical phase [78].

According to Uyar, MTT method measures mitochondrial activity based on the effect of the dehydrogenase activity of intact mitochondria on the reductive cleavage of the yellow tetrazolium salt to a purple formazan compound [83]. In line with this, Uyar et al. purchased six human cancer cells of MCF-7, DLD-1, ECC-1, DU145, PC3, and MDA-MB-231 human cancer cell lines and HEK293 cells from the American Tissue Culture Collection (ATCC, USA), while the supplemented RPMI 1640 medium and DMEM/F-12 were got from Biochrom, USA [83]. Other supplements or antibiotics, such as fetal bovine serum (FBS), fluorouracil (5-FU), L-glutamine, and penicillin/streptomycin (P/S) (100 μg/mL), were purchased from Sigma-Aldrich, USA.

The effect of the Mn(II) compound on the cellular viability was determined using the colorimetric MTT assay. The cells (1×10^5 cells/well) were cultured in a CO_2 incubator with 25 cm^3 tissue culture flasks from Nunc, Denmark, observed consistently under an inverted microscope for any contamination, and subsequently seeded into a 96-well flat bottom microtiter plate. After exposure to various concentrations of compounds for 24 h, cells were washed once with phosphate-buffered saline (PBS) before addition of 100 μL of serum-free medium containing 5 mg/mL of MTT to each well. After incubation for 4 h, the supernatant was removed and the formazan product obtained was dissolved in 100 μL of DMSO of molecular biology grade of >99.9% from Sigma-Aldrich, USA. The cells were cultured in a tissue culture flask in 5% CO_2 incubator, preserved at 37°C in a moistened atmosphere, and observed consistently under an inverted microscope from any contaminations. Each fresh medium was changed every 2 or 3 d until cell convergence was achieved and the cells were isolated by using trypsin EDTA. The mixture was stirred for 20 min on a microliter plate shaker at an absorbance measured at 570 nm with a microplate reader.

Cytotoxicity was expressed as mean percentage increase relative to the unexposed control ± standard deviation (SD). Control values were fixed at 0% cytotoxicity. Cytotoxicity data was fixed to a sigmoidal curve and a four-parameter logistic model was used to calculate the IC_{50}, which is the concentration of material causing 50% inhibition in comparison to the untreated controls. The IC_{50} values were reported at ±95% confidence intervals (±95% CI), and the analysis was performed with GraphPad Prism (San Diego, CA, USA). Cell viability was expressed as the percentage of untreated cells that served as the control group and was labeled as 100% according to the following formula [83]:

$$\%\text{viable cells} = \frac{(\text{the absorbance of the treated cells}) - (\text{the absorbance of the blank})}{(\text{the absorbance of the control}) - (\text{the absorbance of the blank})} \times 100. \quad (2)$$

Concisely, for the MTT assays, Al-anbaky, Li et al., and Li et al. measured cell viability as an indicator of cytotoxicity and, for assessment of compound's toxic effects, Damecheri et al. measured growth inhibition to determine cytotoxicity, and Uyar et al. measured mitochondrial activity to evaluate cytotoxicity [22, 37, 78, 83].

7.2. Sulforhodamine B (SRB) Assay. The reagents required to perform *in vitro* anticancer sulforhodamine B (SRB) assay are RPMI-1640, minimum essential medium (MEM), 10% fetal bovine serum, trypsin, trypan blue, ethanol, penicillin, streptomycin (0.5 mg/mL), dimethyl sulfoxide (DMSO), and sulforhodamine [17]. In addition, a stock solution of 100 μg/mL of all the test compounds was prepared by dissolving in 0.1% DMSO. Subsequently, the compounds were serially diluted and treated to the cancer cells. For cell cultures, the cells were grown and maintained in an appropriate medium, pH 7.4, supplemented with 10% fetal bovine serum (FBM), glutamate (2 mM), penicillin, and streptomycin (0.5 mg/mL). The cell cultures were grown in a carbon(IV) oxide incubator (Heraeus, GmbH, Germany) at 37°C with 90% humidity and 5% CO_2 [17].

According to Khalil et al., the potential cytotoxicity of their synthesized compounds was studied with Skehan and Storeng method [35]. As a result, cells were inoculated with a 96-multiwell plate (104 cells/well) for 24 h before treatment with the synthesized compounds to permit adhesion of the cell to the wall plate. Various concentrations of the synthesized compounds at 0, 5, 12.5, 25, 50, and 100 μg/mL were studied and added to the cell monolayer. Triplicate wells were prepared for each concentration, and the monolayer cells were incubated with the synthesized compounds for 48 h at 37°C and in 5% CO_2 atmosphere. Cells were fixed, washed, and marked with SRB stain, after 48 h.

Acetic acid was used to wash excess stain and the attached stain was recovered with *tris*-ethylenediaminetetraacetic acid

(*tris*-EDTA) buffer [35]. The optical density (O.D.) of each well was measured spectrophotometrically with an ELISA microplate reader at 564 nm. The background mean absorbance was automatically subtracted and mean values of each drug concentration were evaluated. The percentage of cell survival was calculated using the following equation:

$$\text{Survival fraction} = \frac{O.D.\,(\text{treated cells})}{O.D.\,(\text{control cells})}. \quad (3)$$

The triplicate test was to avoid experimental error and to obtain accurate IC_{50} values [35].

Similar to Khalil et al., Ahmed et al., as well as Mohamed and Ahmed, studied the cytotoxicity of their synthesized compounds with SRB assay using Skehan and Storeng method [35, 58, 59].

7.3. Other Assays. There is a challenge of cancer cells' tendency to escape cell death process and frequently exhibiting resistance to treatment by cytotoxic drugs [37]. As a result, novel therapeutic approaches, such as new drugs, are needed to incapacitate cancer cells without harming the normal cells. These new drugs that induce cancerous cell death by apoptosis and autophagy are in high demand. In line with apoptosis, the assays are apoptosis-necrosis assay with flow cytometry analysis and autophagic cell death.

7.3.1. Apoptosis-Necrosis Assay with Flow Cytometry and Cell Death Analyses. Apoptosis is an essential constituent of multistep process of carcinogenesis and resistant cells therapy [37]. It comprises biochemical and terminal morphological events resulting in cell shrinkage, membrane blebbing, chromatin condensation, and membrane-enclosed apoptotic bodies' formation that are phagocytosed to marshal the cellular debris [37]. The apoptotic phases are characterized by DNA fragmentation, mitochondrial membrane integrity loss, and release of molecule for activation initiation of intracellular proteases. The mitochondria play a significant role in the initiation of apoptotic flow by acting as a convergence center of apoptotic signals, as well as the most active organelle for cellular oxidoreductive reactions, which might agree with the mitochondrial membrane potential (MMP) on sternness of the reactive oxygen species (ROS) production [37]. Concisely, mitochondria were considered as a significant factor in the implementation of apoptotic cell death.

Damercheli et al. determined the apoptosis using Annexin V-propidium iodide staining kit according to the manufacturer's recommendations [78]. Annexin V-propidium iodide cells are apoptotic cells, which exist as Annexin V+/PI- and Annexin V+/PI+ cells in the early and late phases [85]. For cell viability assay, the MCF-7 cell line (1×10^5 cells per well) was incubated with the most potent agent ($2\,\mu g \cdot mL^{-1}$) in a 24-well microplate for 24 h which included untreated cells as positive control. Each concentration was tested in duplicate to avoid experimental error [78]. Al-anbanky used the flow cytometry technique to separate apoptotic and necrotic cells, while Damecheri et al. used the flow cytometry technique to perform apoptotic cell death analysis [37, 78].

7.3.2. Autophagic Cell Death. Autophagic cell death (type II programmed cell death) as another cell death pathway emerged as a significant mechanism of cancer cell death induced by chemotherapeutic agents [85]. Autophagy as a "self-cannibalistic" process can behave like a prodeath mechanism leading to cancer cells' death and destruction as a result of defects in apoptosis [85]. Additionally, new perceptions into the molecular mechanisms of autophagy are currently leading to the discovery of inspiring novel potential drug targets [85].

7.4. Apoptosis and Autophagy. Researchers stated that apoptosis and autophagy are firmly connected and might be regulated by the same trigger, such as reactive oxygen species (ROS) [32, 33, 85].

8. Molecular Modelling and Molecular Docking

Computational approach through molecular docking coupled with searching and scoring is one of the most significant approaches for drug design and discovery, which allows molecular interactions and prediction between a ligand and the receptor in the bound state. The two types of docking are protein-protein docking and ligand-protein docking [86]. The protein-protein docking entails two rigid molecules, whose interaction yielded no variation in conformation, while the ligand-protein docking entails a flexible ligand and a rigid receptor protein, whose interaction yielded conformational variations in the ligand. Which docking type does metal complexes belong to? In the case of metal complexes intervention in docking process, they belong to ligand-protein docking. Based on importance, Khalil et al. stated the importance of molecular docking studies to predict the potential binding modes of the most potent compounds with the receptor proteins of breast cancer mutant oxidoreductase whose crystal structure was downloaded from the Protein Data Bank (https://www.rcsb.org/) with identification of PDB ID: 3HB5 [35]. Additionally, Khalil's computational study was aimed at evaluating the binding free energy of the inhibitor inside the macromolecule. However, Gaussian 03 software was used for molecular modelling to build the Schiff base ligand and no Mn(II) was used for computational study.

In Damecheri et al.'s study, the authors used molecular modelling to build the Mn(III) complexes' structural models with HyperChem 8.0 software provided by Hypercube Incorporation (Gainesville, FL (2007)) [78]. As a result, geometric optimization was performed in a two-step procedure which entailed the use of MM + force field as implemented in HyperChem: first the semiempirical method PM3 Hamiltonian with unrestricted Hartree-Fock on the complexes for energy minimization and second the use of RMS gradient of $0.01\,kcal \cdot M^{-1}$ for the full geometry optimization of the complexes [78].

8.1. Molecular Docking Calculations. Khalil et al. used MOE 2008 software for both search algorithm and soring function, which was sourced from Chemical Computing Group Incorporated., Quebec, Canada (2008), to calculate the binding free energy of the inhibitor inside the macromolecule [35]. MOE is an interactive molecular graphics program used to calculate and provide possible docking modes of a receptor and ligand [35]. It required the ligand and the receptor as inputs in PDB format, but Gaussian 03 software was used to create the ligand structure in PDB file format. The crystal structure of B-DNA (PDB ID: 1BNA) was downloaded from the Protein Data Bank (https://www.rcsb.org/). The water molecules, cocrystallized ligands, and other unsupported elements, such as mercury (Hg), potassium (K), and sodium (Na), were removed, while the amino acid chain was retained.

In Damecheri et al.'s study, the rigid molecular docking studies were performed by using MGL tools 1.5.6 with low-resolution Monte Carlo search algorithm of AutoDock4 and the rigid grid box was got using Autogrid (S. Forli. Raccoon AutoDock VS: an automated tool for preparing AutoDock virtual screenings, available from http://autodock.scripps.edu/resources/raccoon) [78]. It was followed by AutoDock with Lamarckian Lamarckian genetic algorithm chosen to perform docking calculations to obtain the best docking conformation. The grid size was set to $72 \times 96 \times 118$ points to cover entire receptor for blind docking with grid spacing of 0.375. Crystallographic water molecules were removed and polar hydrogens and Kollman charges were added to the receptor. The docking was performed in duplicates and the average binding energy was calculated to obtain the scoring function. Default values were set for all other parameters, while the pose with the lowest and best binding affinity was visualized using Schrödinger Maestro.

Concisely, for the two computational studies, Khalil et al. used MOE 2008 software, while Damecheri et al. used MGL tools 1.5.6 with Autogrid4 and AutoDock4 [35, 78].

9. Results and Discussion

In aligning colour with product formation, all researchers reported different levels of brownness for manganese Schiff base coordination compounds in solid (crystals and precipitate) and solution forms.

9.1. Crystallographic Studies. The aforementioned six crystallographic studies entailed factors of different temperatures, absorption corrections, solutions, and refinements software's packages. They were subsequently compared with Müller's standards for crystallographic studies in terms of temperatures, absorption correction, structure solution, and structure refinement.

9.2. Different Temperatures. According to Müller, all diffraction data collection could be at a low temperature such as100 K as a good standard or better at lower temperature than 100 K if possible [87]. This is because, at low temperature, there is reduced atomic movement, which increases the observable resolution, as well as the whole quality and I/σ of the data. The unswerving significance of reduced atomic motion is that low-temperature structures are less affected by disorders. In line with Müller, among the six researchers who studied crystallography of Mn(II) and Mn(III) complexes, Bermejo et al. and Keypour et al. who studied crystallography of Mn(III) complexes did the diffraction data collection at a temperature of 100 K [81, 82, 87]. However, Chang et al., Damercheli et al., Qian et al., and Seck et al. (the other four groups of researchers) who studied crystallography of Mn(II) complexes did the diffraction data collection at temperatures of 298(2) K, 298(2) K, 293 K, and 298(2) K, respectively [75, 78–80]. Müller further stated that crystal structure could be determined at more than one temperature, because occasionally the crystal packing varies as a function of temperature, and this variation is seldom accompanied by noticeable crystal cracking [86]. In line with Müller's further statement, none of the six crystallographic studies reported using more than one temperature [75, 78–82, 87].

9.3. Absorption Correction. According to Müller, the most important statement about absorption correction is that it should always be performed for every crystal, because modern semiempirical methods such as SADABS are not only extremely effective; they also correct for other effects, such as complications arising from crystals that are larger than the primary beam, primary beam intensity variations, and radiation damage [87]. In line with Müller's suggestion on absorption correction, among the six reported crystallographic studies, Damercheli et al. used multiscan methods with Bruker software, Chang et al. used SADABS, Qian et al. used SAINT and SADABS, and Bermejo et al. and Keypour et al. applied Gaussian absorption corrections to their data, but Seck et al. used Lorentz and polarization effects for data correction and did not apply any absorption correction on the reported diffracted manganese complexes' crystals [75, 78–82, 87].

9.4. Structure Solution. According to Müller, numerous small-molecule crystal structures are usually solved by direct methods, such as SHELXS program and SIR program, which are in most cases very successful methods [87]. However, for the few cases when direct methods fail, Patterson methods might suitably work particularly with a few heavier atoms in the molecule. In line with Müller's statements on structure solution, none of the six crystallographic studies reported the use of Patterson method [75, 78–82, 87]. However, Damercheli et al. used SIR2004 program, while the other five crystallographic studies reported the use of direct method of SHELXS for structures "solutions on the diffracted manganese complexes" crystals [75, 78–82].

9.5. Structure Refinement. Müller defined structure refinement as a process of iterative variation of the molecular model aimed at maximizing its agreement with the diffraction data [87]. All the six crystallographic studies reported the use of full-matrix least-square methods based on F2 for structure refinements [75, 78–82]. All the

nonhydrogen atoms on F2 were anisotropically refined anisotropic thermal parameters using SHELXL software package program, while the hydrogen atoms in the crystals of the Mn complexes were all located from difference Fourier maps, and residual hydrogen atoms were fixed with thermal parameters and placed at geometrical positions. Damercheli et al., Seck et al., and Keypour et al. further stated the use of riding model to refine the hydrogen atoms at the geometrical positions [78, 80, 82].

9.6. Synthesis of Manganese Schiff Base Coordination Compounds and Their Anticancer (Cytotoxic) Studies. Manganese has applications as therapeutic and anticancer agents [31–33, 84, 88]. On a superior note, *in vivo* Mn(II)'s transport mechanism might make Mn(II)-based compounds possible tumor targets, but ethics based on animal protection might give it a reconsideration for computational studies [85, 89]. Some Mn(II) salts were reported to apply antiproliferative actions on various cancer cell lines usually by apoptotic and autophagic cell death [85].

9.6.1. Cytotoxic Activity Evaluation with MTT Assay. In recent times, an innovative strategy for the effective antitumor compounds' development was Mn(II) combination with other functional molecules, such as ligands. This section has eight groups of researchers who used MTT assay.

9.6.2. Li et al.'s Cytotoxic Study Using MTT Assay. The LMnAc showed significant selectivity towards Hep-G2 over WRL-68 in comparison with cisplatin towards cancer cells over noncancer cells [24]. Concisely, LMnAc is a prospective anticancer agent.

9.6.3. Haque et al.'s Study. In line with this regency, Haque et al. studied the cytotoxic activities of five synthesized novel ferrocene Schiff base metal complexes, namely, $[Mn(Fcd)(COO)_2]$, $[Co(Fcd)(COO)_2]$, $[Ni(Fcd)(COO)_2]$, $[Cu(Fcd)(COO)_2]$, and $[Zn(Fcd)(COO)_2]$ [76]. An *in vivo* method with brine shrimp bioassay was used to measure the cytotoxic activities. For probit analysis and simplest estimation, as regards LC_{50} (lethal concentration), results were not obtained with a software program but through calculation with a regression equation. Probit analysis is a type of regression used to analyze binomial response variables. None of the metal complexes had superior cytotoxic activity than the two standards (bleomycin and garlic acid) used as positive controls. However, among the five metal complexes, $[Mn(Fcd)(COO)_2]$ showed the highest cytotoxic effect with LC_{50} of 8.14 ppm as given in Table 1 [76].

9.6.4. Chang et al.'s Study. Chang et al. did the *in vitro* cytotoxicity cell culture studies as a general method to screen three samples for their anticancer drug potentials and to understand the anticancer activities with the MTT method [75]. Chang et al. reported the IC_{50} of the cytotoxic activities for the three metal complexes to be higher and more potent than that of cisplatin for all the three cancer cell lines [78]. The copper complex, [Cu(ONO-(R)L2)]4.2CH3OH, had a less cytotoxic activity than [Mn3(ONO-(S)L3)4(OAc)4(H2O)2][Mn3(S-L3)4(OAc)4(H2O)2] with the exception of MDA-MB-231 cancer cell line but better cytotoxic activity than manganese(II) complex, [Mn(ONO-(S)L1)2], for all the three metal complexes. The lower IC_{50} values of trinuclear manganese complex 3 showed better cytotoxic inhibitory effects than its corresponding mononuclear complex 1 for A549 and HeLa cancer cell lines (Table 2) [75].

9.6.5. Damercheli et al.'s Study. Damercheli et al. synthesized four manganese(III) Schiff base complexes [78]. The Schiff base ligands were products from condensation reaction which involved meso-1,2-diphenyl-1,2-diphenyl-1,2-ethylenediamine and salicylaldehyde or its 3-OMe-, 5-Br-, or 5-OMe- derivatives (where $x = 1$–4) as shown in Scheme 1 and Table 3, respectively [78]. The *in vitro* anticancer activities of the coordination compounds were screened using apoptosis and MTT (3-(4,5-dimethylthiazol-2yl)-2,5-diphenyltetrazolium bromide) assay against human breast (MCF-7) and liver (Hep-G2) cancer cells. The IC_{50} results for the studied samples against two anticancer cell lines (MCF-7 and Hep-G2) are given in Table 4. The IC_{50} is defined as the concentration of an inhibitor where the response is reduced by half testing viability via an MTT assay [88]. In other words, the dose of cytotoxic compound where 50% viability is achieved is the IC_{50} when testing viability through an MTT assay [88, 89]. Concerning the IC_{50} standard for cytotoxic samples, the Mn(II) coordination compounds belong to the active cytotoxic category because the IC_{50} value occurs less than 100 μg/mL based on Prayong classification [77]. Damercheli et al. concluded that the complexes showed considerable anticancer activities against both cell lines ($IC_{50} = 10.8$–$21.02\,\mu$M) as given in Table 4 [78]. The highest anticancer activity was found for $[MnClL^1]$ with IC_{50} results of 14±1 mM and 11±1 mM in both MCF-7 and Hep-G2, respectively. In comparison with the standard drug (cisplatin), $[MnClL^1]$ has a better IC_{50} cytotoxic value.

9.6.6. Liu et al.'s Study. In Liu et al.'s study, the antitumor activity of the novel manganese(II) compound, Adpa-Mn [(Adpa)Mn(Cl) (H_2O)] (Adpa = bis(2-pyridylmethyl) amino-2-propionic acid), with possible reaction mechanisms was investigated [84]. The *in vitro* growth inhibitory effects of Adpa-Mn with IC_{50} values lower than 15 μM on tumor cell lines were examined by MTT assay. They discovered that the compound was more selective against cancer cells than cisplatin (the popular chemotherapeutic reagent). In addition, they discovered that Adpa-Mn attained its selectivity against cancer cells via the transferrin-(Tf-) transferrin receptor (TfR) system, which is highly conveyed in tumor cells. I*n vivo*, the induction of apoptosis and autophagy in tumor tissue was confirmed after treatment with Adpa-Mn, which impacted its significant antitumor activity against hepatocellular carcinoma (Hep-A cell) xenografts at 10 mg/kg. The eight cancer lines used are

Table 2: The IC_{50} (μM) results for the in vitro cytotoxic activities for three compounds screened against lung cancer (A549), cervical carcinoma (HeLa), and breast cancer MDA-MB-231 cell lines.

Metal complex	A549	HeLa	MDA-MB-231
[Mn(ONO-(S)L1)2]	34.63 ± 1.54	38.73 ± 1.59	46.85 ± 1.67
[Cu(ONO-(R)L2)]4.2CH3OH	29.68 ± 1.47	17.94 ± 1.25	6.20 ± 0.79
[Mn3(ONO-(S)L3)4(OAc)4(H2O)2][Mn3(S-L3)4(OAc)4(H2O)2]	21.91 ± 1.36	10.54 ± 1.02	18.42 ± 1.27
Cisplatin	>60	>60	>60

A549, lung cancer cell line; HeLa, cervical carcinoma cell line; MDA-MB-231, breast cancer cell line; cisplatin, positive control.

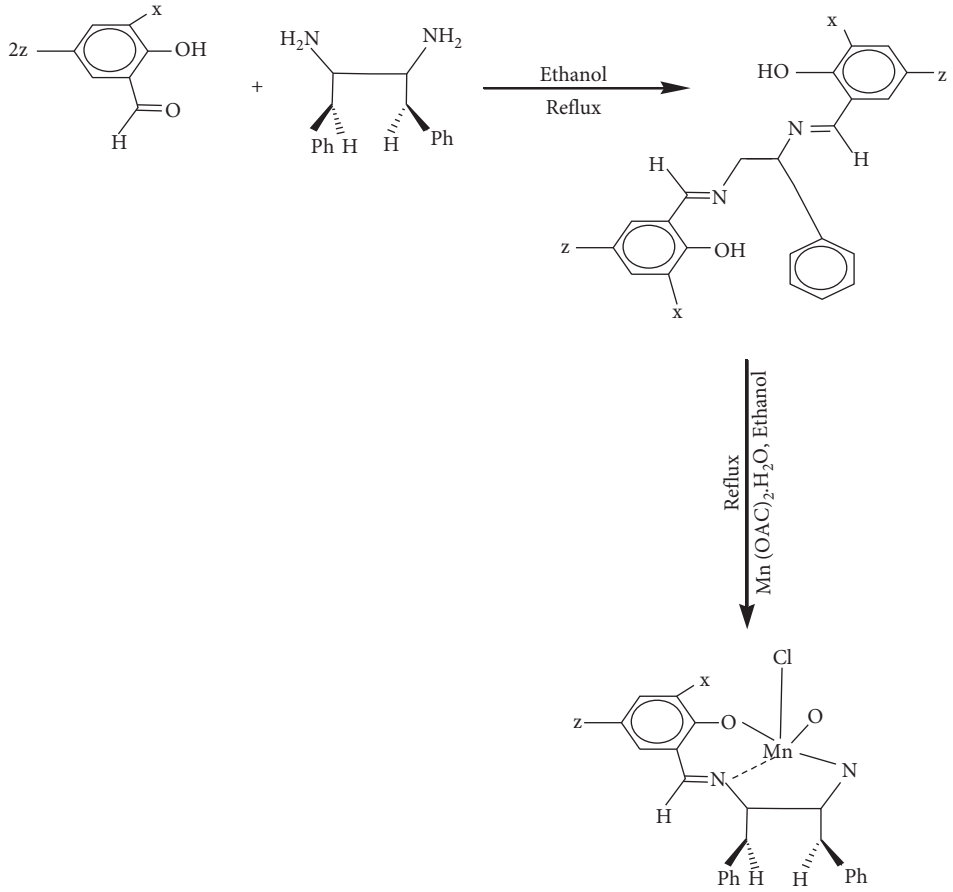

Scheme 1: Synthesis of ligand and manganese(II) complex [78].

Table 3: Damercheli et al.'s four novel manganese(III) Schiff base complexes.

Ligands	Complexes	X	Z
H_2L^1	$[MnClL^1]$	H	H
H_2L^2	$[MnClL^2]$	OCH_3	H
H_2L^3	$[MnClL^3]$	H	Br
H_2L^4	$[MnClL^4]$	H	OCH_3

human cervical cancer cells (HeLa), human hepatocellular carcinoma cells (Hep-G2), human lung cancer cells (A549), human breast cancer cells (MCF-7), human glioblastoma cells (U251), human colon cancer cells (LoVo), human melanoma cells (A875), and human esophageal squamous carcinoma cells (ECA-109) as given in Table 5 [84].

Table 4: The IC_{50} results for studied samples against two anticancer cell lines (MCF-7 and Hep-G2).

Samples	IC_{50} (mM) ± SD	
	MCF-7	Hep-G2
L^{1-4}	>100	>100
$[MnClL^1]$	14 ± 1	11 ± 1
$[MnClL^2]$	16 ± 1	12 ± 1
$[MnClL^3]$	16 ± 1	12 ± 1
$[MnClL^4]$	21.0 ± 0.5	16 ± 1
Cisplatin	20 ± 1	38.3 ± 0.7

IC_{50}, inhibition concentration; SD, standard deviation of the results.

9.6.7. Uyar et al.'s Study. Similarly, Uyar et al. reported IC_{50} cytotoxic activities of six manganese(III) complexes above 100 μM against six different cell lines as given in Table 6 [83].

Table 5: Half maximal inhibitory concentration (IC_{50}) of Adpa-Mn in eight cancer cell lines.

Cell line	IC_{50} (M)
HeLa	12.3 ± 1.5
Hep-G2	10.8 ± 0.9
A549	14.2 ± 0.5
MCF-7	6.5 ± 0.7
U251	9.1 ± 0.6
LoVo	10.2 ± 0.4
A875	18.6 ± 0.3
ECA-109	16.2 ± 0.3

Table 6: The IC_{50} results for the in vitro cytotoxic activities of ligand, Cu(II) complex, and Mn(II) complex and 5-FU screened against six cancer cell lines.

Cell lines	IC_{50} values (μM)			
	Ligand	Cu(II) complex	Mn(II) complex	5-FU
MCF-7	>1000	43.4	273.6	58.44
DLD-1	219.4	142.9	193.8	39.34
DU-145	177.2	93.5	182.9	50.22
ECC-1	386.9	100	304.8	34.4
HEK293	327.8	398.8	373.1	24.33
MCF-7	>1000	43.4	273.6	58.44
MDA-MB231	176.6	129	187.8	62.33
PC3	310.5	63.2	117.3	55.44

Light red, low activity; yellow, moderate activity; green, high activity.

Uyar et al. reported the cytotoxic activities of the Schiff bases of copper(Cu)II complex and Mn(II) complex, when screened against MCF-7, DLD-1, ECC-1, DU-145, PC3, and MDA-MB231 cancer cell lines and HEK293 normal cell line for 24 h as given in Table 6. Cell viability curves were used to analyze the results and expressed as IC_{50} values in a concentration range from 0 to 200 μM. The half-maximal inhibitory concentration (IC_{50}) was defined as the concentration required to reduce the size of the cell population by 50% [83]. The IC_{50} values obtained for ligand and its complexes against the tested cell lines are given in Table 6. Fluorouracil (5-FU) was used as standard (positive control). By assessing and comparing the IC_{50} values, copper complex showed higher cytotoxicity compared to the ligand and the manganese complex. The IC_{50} values for the eight Mn(II) complexes were of either low or moderate cytotoxic activities.

9.6.8. Shen et al.'s Study. In the case of Shen et al., the authors developed four anticancer agents, which comprised a Schiff base, E-N'-(1-(pyrindin-2-yl)ethylidene) nicotinohydrazide (penh), and four metal ions (Mn^{2+}, Co^{2+}, Cu^{2+}, and Cd^{2+}) to synthesize $[Mn(penh)_2]$, $[Co(penh)_2]$, $[Cu(penh)_2]$, and $[Cd(penh)_2]$ [89]. The *in vitro* cytotoxic activities were assessed using MTT assay against three anticancer cell lines, namely, human lung cancer (A549), human gastric cancer cell line (BGC823), and human esophageal cancer (109) cell lines [90]. In comparison with the parent penh ligand, all the four metal complexes were able to distinctly reduce the proliferation rate of the three anticancer cell lines in a concentration-dependent way (Table 7) [90]. It could be observed that $[Mn(penh)_2]$ had less cytotoxic activity against A549, BGC823, and Eca109 cancer cell lines when compared with cytotoxic activities of $[Co(penh)_2]$ and $[Cu(penh)_2]$ as given in Table 7 [90]. On another note, $[Mn(penh)_2]$ gave a lesser cytotoxic result for BGC823 cancer line and better cytotoxic result for A549 and ECA-109 cancer cell lines than $[Cd(penh)_2]$.

Table 7: Half-maximal inhibitory concentration (μmol/l) results for the parent E-N'-(1-(pyrindin-2-yl)ethylidene) nicotinohydrazide ligand and four metal complexes against three anticancer cell lines, namely, human lung cancer (A549), human gastric cancer cell line (BGC823), and human esophageal cancer (ECA-109) cell lines.

Compound	EC_{50} (μmol/l)		
	A549	BGC823	ECA-109
Ligand	156.5	196.8	165.1
$[Cd(penh)_2]$	13.5	15.6	11.9
$[Co(penh)_2]$	8.1	11.8	10.3
$[Cu(penh)_2]$	7.3	9.7	6.5
$[Mn(penh)_2]$	12.2	18.3	9.6

9.6.9. Gwaram and Hassandarvish Combined Study. Gwaram and Hassandarvish synthesized Schiff base 2-(1-(2-morpholinoethylimino)ethyl)phenol (L_g) from the condensation reaction of 2-hydroxyacetophenone with 4-(2-aminoethyl) morpholine with few drops of glacial ethanoic acid to regulate the pH as shown in Scheme 2 [91].

MTT Assay. Gwaram and Hassandarvish also used MTT assay to determine the cytotoxic activities of ten studied compounds against MCF-7 breast cancer cell line [91]. The studied compounds showed active cytotoxicity mediated on MCF-7 and were selective to some extents when compared with WRL68 normal liver cell line. The assay functioned as an index applied in determining cytotoxicity of the studied compounds to arouse or inhibit cell viability and growth by identifying the decrease of tetrazolium salt to form formazan by mitochondrial enzyme activity of succinate dehydrogenase [91]. Results from the MTT assay showed that the free ligand exhibited no significant inhibition activity which confirmed that the chelation of the Schiff base with metal (II) ions was significant for the anticancer activities of the new compounds as given in Table 8 [91]. Apart from a higher cytotoxic result of Cu(LI)Br (4.25 μg/mL) compared to Mn(LI)Br (5.93 μg/mL), Mn(LI)Br had better cytotoxic activity than the other bromo-substituted coordination compounds, Zn(LI)Br (33.09 μg/mL) and Ni(LI)Br (27.64 μg/mL). For the comparison of the bromo-substituted and chloro-substituted manganese Schiff base coordination compounds, for both MCF-7 and WRL68 cancer cell lines, the EC_{50} results of Mn(LI)Br with 5.93 μg/mL and 4.65 μg/mL were more active and more cytotoxic to the two cancer cells, respectively, than the Mn(LI)Cl with 24.54 μg/mL and 44.25 μg/mL.

9.6.10. Alturiqi et al.'s Study. Alturiqi et al. synthesized coordination compounds of Cr(III), Ru(III), Mn(II), Co(II), Ni(II), Cu(II), and Zn(II) from furan ligand (5-hydroxymethylfuran-2-yl-methyleneaminoquinolin-2-one; H-MFMAQ) derived from

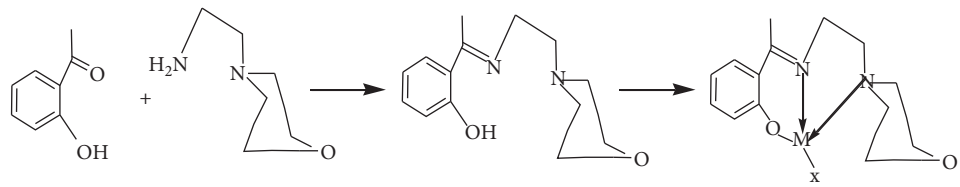

Where M= Cu, Zn, Ni or Mn

X= Cl^- or Br^-

Scheme 2: Synthesis of Schiff base ligands and its corresponding metal(II) coordination compounds [91].

Table 8: The EC_{50} results in μg/mL for ten studied compounds on MCF-7 and WRL68 and cancer cell lines.

Compounds		EC_{50} μg/mL	
		MCF-7	WRL68
1	L1	n.d	n.d
2	Cu(LI)Br	4.25	28.28
3	Cu(LI)Cl	37.58	41.15
4	Mn(LI)Br	5.93	4.65
5	Mn(LI)Cl	24.54	44.25
6	Ni(LI)Br	27.64	64.53
7	Ni(LI)Cl	8.15	13.05
8	Zn(LI)Br	33.09	52.26
9	Zn(LI)Cl	10.94	32.69
10	Cisplatin	2.50	—

the condensation of 5-hydroxymethylfuran-2-carbaldehyde and 1-aminoquinolin-2(1H)-one [92]. All tested compounds were screened against human breast (MCF-7) and lung (A549) cancer cell lines for their cytotoxic activities as shown in Table 9. The Mn(II) complex had less active cytotoxicities for both cancer cell lines when compared to the cisplatin (standard drug) but more active cytotoxicities than the parent ligand for both cancer cell lines. In the case of MCF-7 cancer cell line, Mn(II) complex had less cytotoxicity when compared with Co(II), Cr(II), Ni(II), and Ru(II) complexes but had higher cytotoxicity when compared with Cu(II) and Zn(II) complexes. In the case of A549 cancer cell line, Mn(II) complex has less cytotoxicity when compared with Co(II), Cr(II), and Ru(II) complexes but has higher cytotoxicity when compared with Ni(II), Cu(II), and Zn(II) complexes for both MCF-7 and A549 cancer cell lines. In comparison with Khalil et al.'s study, for both MCF-7 and A549 cancer cell lines, Mn(II) had less IC_{50} values than cisplatin and better IC_{50} values than the ligand [35, 92] (see Table 10)

IC_{50} is the concentration of compounds required to inhibit growth of 50% of the cancer cells (μM). The data is mean ± standard deviation (SD) of three replicates.

In summary, from the eight groups of researchers who reported using MTT assay as *in vitro* and *in vivo* technique to determine the cell viability and growth inhibition via cytotoxic activities, Haque et al. reported that $[Mn(Fcd)(COO)_2]$ with LC_{50} value of 8.14 ppm showed the highest cytotoxic effect among the five metal complexes $[Co(Fcd)(COO)_2]$, $[Cu(Fcd)(COO)_2]$, $Mn(Fcd)(COO)_2]$, $[Ni(Fcd)(COO)_2]$, and $[Zn(Fcd)(COO)_2]$ [76].

In the case of Damercheri et al.'s study, $[MnClL^1]$ with IC_{50} values of 14 ± 1 mM and 11 ± 1 mM in both MCF-7 and Hep-G2, respectively, had higher cytotoxic activities than cisplatin and the other three Mn(II) complexes with at least a substituent (Br or OCH_3) [78]. The reason for $[MnClL^1]$'s highest cytotoxic activities might be due to it having no substituent status, while others have meta- and para-substituent positions [78]. Chang et al. studied *in vitro* cytotoxicities of mononuclear Mn(II), mononuclear Cu(II), and trinuclear Mn(II) complexes [75]. They discovered that, with the exception of MDA-MB-231 breast cancer cell line, trinuclear Mn(II) complex had the best cytotoxic results. From Chang et al.'s study, there is an indication that manganese's nuclearity plays a significant role in the cytotoxicity (anticancer) activity of the Mn(II) complexes. In Liu et al.'s study, *in vitro* growth inhibitory effects of Adpa-Mn with IC_{50} value of 6.5 ± 0.7 μM was highest when tested against MCF-7 cancer cell line among eight cancer cell lines. Similar to Liu et al.'s study, Uyar et al.'s study entailed seven Mn(II) complexes against seven cancer cell lines. The obtained IC_{50} values for Mn(II) were of either low or moderate cytotoxicities. Chang et al.'s method might be applied to Mn(II) by making the mononuclear manganese complexes

Table 9: Cytotoxicities (IC_{5O}, μM) of Schiff base ligand, seven metal complexes, and cisplatin.

Compound	MCF-7	A549
Ligand	25 ± 1.2	28 ± 1.4
Co(II) complex	19 ± 1.7	22 ± 1.9
Cr(III) complex	17 ± 1.6	20 ± 1.7
Cu(II) complex	26 ± 1.5	37 ± 0.8
Mn(II) complex	21 ± 1.6	24 ± 1.6
Ni(II) complex	21 ± 1.7	28 ± 1.4
Ru(II) complex	18 ± 1.5	21 ± 1.7
Zn(II) complex	29 ± 1.7	38 ± 1.2
Cisplatin	13 ± 0.5	12 ± 0.9

Table 10: The cytotoxic activities (μg/ml) of Schiff base ligand and its Mn(II) and La(III) complexes at different concentrations against the MCF-7 cell line.

Compound	Surviving fraction (MCF-7) Concentration (μg/ml)					IC_{50} (μg/ml)
	0	5	12,5	25	50	
L	1	0.746	0.560	0.522	0.410	29
Mn(II)	1	0.784	0.597	0.410	0.373	20
La(II)	1	0.933	0.896	0.672	0.485	48

trinuclear [75]. In Shen et al.'s study, $[Mn(penh)_2]$ had less cytotoxic activities against A549, BGC823, and ECA-109 cancer cell lines when compared with cytotoxic activities of $[Co(penh)_2]$ and $[Cu(penh)_2]$ [89]. There could be an improvement with Chang et al.'s method by making the mononuclear $[Mn(penh)_2]$ complexes trinuclear. Gwaram and Hassandarvish studied ten studied compounds against MCF-7 breast cancer cell line and compared with WRL68 normal liver cell line [88]. In comparison between MCF-7 cancer cell line and WRL68 normal liver cell line, Mn(LI)Br had better cytotoxic activity when tested against MCF-7 cancer cell line than WRL68 normal liver cell line. Chang et al.'s method might be applied to Mn(II) by making the mononuclear manganese complexes trinuclear to obtain enhanced cytotoxicities (IC_{50} values) for the Mn(II) complexes.

Alturiqi et al. tested their compounds against human breast (MCF-7) and lung cancer (A549) cell lines for their cytotoxic activities as shown in Table 9 [92]. The Mn(II) complex had less active cytotoxicities for both cancer cell lines when compared to cisplatin (standard drug) but more active cytotoxicities than the parent ligand with respect to both cancer cell lines. In the case of MCF-7 cancer cell line, Mn(II) complex had less cytotoxicity when compared with Co(II), Cr(II), Ni(II), and Ru(II) complexes but had higher cytotoxicity when compared with Cu(II) and Zn(II) complexes. In the case of A549 cancer cell line, Mn(II) complex had less cytotoxicity when compared with Cu(II), Ni(II), and Zn(II) complexes but had higher cytotoxicity when compared with Ni(II), Cu(II), and Zn(II) complexes. Mn(II) complex had better and higher cytotoxic activity against human breast cancer (MCF-7) cell line than the Schiff base ligand (SBL).

9.7. Cytotoxic Activity Evaluation with SRB Assay. For SRB assay, three groups of researchers' studies were considered.

9.7.1. Khalil et al.'s Study. In Khalil et al.'s study, the cytotoxic activities of Schiff base ligand and its Mn(II) and La(III) complexes were screened against the MCF-7 cell line (breast carcinoma cells) [35]. As a result, all the synthesized compounds were examined against single-dose 100 μg/ml of MCF-7 cell line with Skehan and Storeng method. The *in vitro* screening of the synthesized compounds showed that the Schiff base had good anticancer 65% inhibition activity, while Mn(II) complex showed higher inhibition of about 67% than that of the parent Schiff base ligand and other complexes. The La(III) complex had also a good anticancer activity (63% inhibition) but it was less than that of the parent Schiff base ligand. The half-inhibitory concentration (IC_{50}) values and the mode of anticancer activity were assessed with various concentrations (5, 12.5, 25, and 50 μg/ml), and the data obtained are shown in Table11. The Mn(II) complex showed the lowest IC_{50} value at 20 μg/ml, which indicated higher efficiency against breast carcinoma cells than the parent Schiff base ligand (SBL) and La(II) complex [35].

9.7.2. Ahmed et al.'s Study. Ahmed et al. studied the *in vitro* anticancer activities of L, $[Cr(L)\ (H_2O)_2Cl]Cl_3{\cdot}2H_2O$, and $[Cr(L)\ (H_2O)_2Cl]Cl_3{\cdot}2H_2O$ at different concentrations against MCF-7 breast cancer cell lines with Skehan and Storeng method [58]. The results with their obtained IC_{50} values are shown in Table 12. In comparing the IC_{50} values of ligand, Cr(III), and Mn(II) complexes, it was discovered that the Mn(II) complex had higher cytotoxic activity against human breast cancer cells (MCF-7) than the ligand and $[Cr(L)\ (H_2O)_2Cl]Cl_3{\cdot}2H_2O$ complexes.

9.7.3. Mohamed and Ahmed's Combined Study. Mohamed and Ahmed prepared Schiff base ligand (SBL) by the condensation reaction of 2,2-(ethylenedioxy)bis(ethylamine) and imidazole-2-carboxaldehyde in a 1:2 ratio, and the seven metal complexes of Cd(II), Cr(III), Cu(II), Fe(III), Mn(II), Ni(II), and Zn(II) ions were synthesized in a ratio of 1 SBL to 1 metal ion (1:1 ratio) [59]. Characterization techniques used to identify the Schiff base ligand and metal complexes are BET surface area, elemental analysis, magnetic properties, molar conductivity, infrared, proton (^{1}H) NMR spectral tests, theoretical DFT, thermal analysis, and UV which were used to identify the metal complex structures. For all the metal complexes, the ligand behaved as a neutral tetradentate ligand with N_2O_2 donor atoms and spectroscopic studies indicating an octahedral structure. The Mn(II) complex had higher cytotoxic activity against human breast cancer cell line (MCF-7) than the Schiff base ligand (SBL) and five metal complexes, with the exception of $[Cu(H_2L)Cl]Cl{\cdot}2H_2O$, as shown in Table 11.

In summary, in Khalil et al.'s and Ahmed et al.'s studies, the Mn(II) complex showed the highest cytotoxic activity with IC_{50} value of 20 μg/ml and IC_{50} value of 21 μg/ml, which indicated higher efficiencies against MCF-7 breast cancer cells than the parent Schiff base ligand (SBL), La(II), and Cr(II) complexes [35, 58]. In the case of Mohamed and Ahmed's study, the Mn(II) complex had higher cytotoxic activity against human breast cancer cell line (MCF-7) than the Schiff base ligand (SBL) and five metal complexes, with the exception of $[Cu(H_2L)Cl]Cl{\cdot}2H_2O$ [58, 59]. Chang et al.'s study could be applied to the Mn(II) complex for enhanced IC_{50} result [75]. For Ahmed et al.'s study, the Mn(II) complex had higher cytotoxic activity against human breast cancer cells (MCF-7) than the ligand [58].

9.8. Other Assays

9.8.1. Adpa-Mn and Induction Autophagic Cell Death Apoptosis-Necrosis Assay with Flow Cytometry Analysis. Li et al. explored the inhibition essentials of their earlier identified novel synthesized manganese(II) compound, LMnAc ([L2Mn2(Ac) (H2O)2](Ac) (L = bis(2-pyridylmethyl) amino-2-propionic acid) induced cancer cell [24]. Their study revealed that LMnAc used transferrin-transferrin receptor system to achieve its selectivity against cancer. The process being facilitated with the mitochondrial pathway involved LMnAc triggering the cancer cells to induce autophagy and apoptosis. Additionally, LMnAc

Table 11: Anticancer effects of Schiff base ligand and its metal complexes in % cell inhibition at 100 μg/ml concentration.

Samples	% cell inhibition	Surviving fraction (MCF-7)					IC_{50} (μg/ml)
		0.0	5.0	12.5	25	50	
H_2L	64						—
$[Cd(H_2L)\ (H_2O)Cl_2]$	64						—
$[Cr(H_2L)(H_2O)_2Cl]Cl_2{\cdot}2H_2O$	64						—
$[Cu(H_2L)Cl]Cl{\cdot}2H_2O$	70	1	1	0.73	0.33	0.31	19.6
$[Fe(H_2L)(H_2O)_2Cl]Cl_2$	75	1	0.88	0.71	0.64	0.25	33
$[Mn(H_2L)(H_2O)_2Cl]Cl{\cdot}2H_2O$	72	1	0.85	0.73	0.51	0.33	26
$[Ni(H_2L)(H_2O)]Cl_2{\cdot}4H_2O$	75	1	0.88	0.81	0.62	0.3	34
$[Zn(H_2L)(H_2O)Cl_2]{\cdot}2H_2O$	67						—

Table 12: Anticancer effects of Schiff base ligand and its metal complexes of % cell inhibition at different concentrations against MCF-7 breast cancer cell line.

Samples	% cell inhibition	Surviving fraction (MCF-7)					IC_{50} (μg/ml)
		0.0	5.0	12.5	25	50	
L	67	1	0.95	0.85	0.61	0.23	31
$[Cr(L)\ (H_2O)_2Cl]Cl_3{\cdot}2H_2O$	67	1	0.95	0.71	0.46	0.25	23
$[Mn(L)\ (H_2O)Cl]Cl{\cdot}3H_2O$	70	1	0.8	0.75	0.38	0.28	21

interrupted mitochondrial function to bring about mitochondrial membrane potential (MMP) collapse and adenosine triphosphate (ATP) reduction [24]. The LMnAc also induced intracellular Ca2+ overload and reactive oxygen species generation. Remarkably, its anticancer effect was significantly reduced, and subsequent pretreatment with the antioxidant N-acetyl cysteine indicated that reactive oxygen species (ROS) triggered cell death. Concisely, their data recommended LMnAc as a selectively promising anticancer drug candidate.

In the case of Al-anbaky et al.'s study, the authors used the most common cytotoxic assays to assess general cytotoxicity involving a widely used model cell line for human breast cancer [37]. Subsequently, they integrated the nucleic acid-binding fluorochromes ethidium bromide/acridine orange (EB/AO) to examine and determine the cell viability and apoptosis of the MCF-7 cells via fluorescence microscopy EB/AO and flow cytometry to ascertain whether the cytotoxic effects of the Mn(III) complex were mediated by apoptotic events. Their study was mainly selected with YO-PRO-1 Vybrant apoptosis assay to identify membrane integrity variations that triggered early and late apoptotic events, as well as cells undergoing necrotic death. Both YO-PRO-1and Annexin V detect changes in orientation of phospholipids in plasma membrane but YO-PRO-1 seems to be more sensitive and more widely applied in complex systems of flow cytometry.

Mitochondrial integrity was measured by ROS production and changes in MMP. Results showed that the Mn(II) complex synthesized and characterized by our group mediates cytotoxicity using both apoptotic and necrotic cell death mechanisms [37]. The Adpa-Mn induction of autophagy was analyzed with autophagic vacuole organelle (AVO) formation, formation of green fluorescent protein-light chain 3 (GFP-LC3) vacuoles, and light chain 3 (LC3) conversion to determine if autophagic cell death contributes to the cytotoxic effects of Adpa-Mn [84]. The result showed that the Adpa-Mn-treated hepatocellular carcinoma (Hep-G2) cells had a greater fluorescence intensity and a greater number of monodansylcadaverine- (MDC-) labeled particles compared with the control (untreated) group, indicating that Adpa-Mn improved MDC mobilization to autophagosomes in the cytoplasm which was repressed by the autophagy inhibitor, 3-Methyladenine (3-MA) [84].

10. Structure-Based Drug Design, Virtual Screening, and Molecular Docking Activities

Three-dimensional (3D) models of creating chemical structures are single X-ray crystallography and nuclear magnetic resonance (NMR) [93]. These 3D models are used to describe the positions of the atoms that compose the manganese Schiff base complexes in alignment with the "lock and key" analogy for drug action. Between the three-dimensional models of chemical structures, this study earlier focused on single X-ray crystallography. As a result, single X-ray crystallography is an experimental technique used to determine the coordinate information of the atoms in the manganese Schiff base complexes and their surroundings. However, in computational medicinal chemistry, structure-based drug design and virtual screening (VS) are areas that use three-dimensional (3D) models of target proteins aimed at increasing the speed and quality of early stage drug discovery [93]. Generally, VS is used to screen group of patented compounds aimed at selecting and testing compounds for their biological activities [93]. The focus has been to include as many active compounds as possible among those selected for testing. Essentially, the three categories of VS methods are ligand-based virtual screening (LBVS), which depends on the activity information of one or more standards (known compounds); structure-based virtual screening (SBVS), which uses structural target information; and combined methods, which used information obtained from both ligands and target structure [93]. In SBVS, diverse

types of information about the targets (manganese Schiff base complexes, or usually a protein (cancer cell line)) are used. Techniques such as interaction fingerprints or pharmacophores could be based on target information, but the topmost technique is docking. Docking could be defined as the prediction of the bioactive conformation of a molecule (ligand) in the binding site of a target structure [58, 78, 93]. This is similar to discovering the minimum Gibb's free energy of a protein-ligand system. In other words, docking involves the placement of a compound or ligand within the protein and scoring this position or pose according to the change in energy [78, 93]. Docking is used to virtually screen novel compounds similar to experimental high-throughput (HTP) screening, as well as offering microscopic understanding to ease structure-based drug design [94]. It is aimed at predicting and discovering stable binding conformations between a ligand and a receptor, that is, accurate data modelling and ligand activity prediction [93]. In other words, docking experiments are performed to successfully study the molecular binding behaviour of metal complexes with receptors. The purpose is to promote green chemistry, reduce the cost of effectual screening of large database of chemical compounds used for drug design and drug discovery, explore harmful laboratory chemicals virtually by simulation, and save time [93]. The three-dimensional (3D) structures of metal complexes such as manganese complexes are regarded as ligands, which could be modelled with software, such as MarvinSketch, and the docking studied with a combination of AutoDock4 and the genetic algorithm method. However, there are various types of receptors (proteins) in the Protein Data Bank (PDB), void, or with the relevant and right ligand (drug). According to Ainsley et al., customary lead generation methods for drug discovery generally entail assaying a large diversity of interesting compounds against a specific protein known to be a disease target with the hope to observe a binding interaction [93]. Ahmed et al. defined molecular docking as a valuable technique to predict the stable structure of receptor-ligand complex for improved recognition of the interaction details in drug discovery process [58]. This method is often used as virtual (computer-generated) searching tool in main steps of drug discovery, design, and development [58]. Khalil et al. implemented docking studies to predict the binding modes of Schiff base ligand with receptor of breast cancer mutant oxidoreductase (PDB ID: 3HB5) [35]. The result revealed that the main interaction forces of Schiff base ligand with the active sites were H-donor and H-acceptor. The lowest binding energies for Schiff base ligand were found to be −1.2 kcal/mol with 3HB5. Prior to molecular docking, Danercheli et al. used molecular modelling via Hyperchem 8.0 software to generate the three dimensional structures of the metal complexes. In molecular docking, the two criteria modules are the search algorithm and scoring function. For the search algorithm, Damercheli et al. used AutoDock as a low-resolution Monte Carlo search used Au [94]. For the scoring function, Damercheri et al. used active site waters and calculated binding Gibb's free minimization energy, desolvation energy components of calculated docking energies, electrostatic interactions of individual metal complex in the active site of the associated targets, hydrophobic interaction, hydrogen bonds, solvation effects, and Van der Waal's interactions for the Mn(II) complexes-receptor targets. In other words, among the four Mn(II) complexes, the parent complex of Mn(III) series, [MnClL1], presented diverse binding modes when compared with the other three Mn(III) derivatives [94].

11. Conclusion

This study reviews the significance and application of Schiff base as the right ligand to overcome Mn ion's challenges of bioavailability and neurogenerative toxicity to achieve manganese Schiff base coordination compounds in fulfilment of chelation therapy, as well as being key anticancer agents. Among the variable oxidation states of human biologically inclined Mn (+2, +3, and +4), this study focused more on the manganese(II) Schiff base coordination compounds than on the manganese(III) and manganese(IV) Schiff base coordination compounds due to the most available literature on it. Additionally, there was more of the use of MTT bioassay as cytotoxic method than sulforhodamine B. Most researchers reported more of *in vitro* and less of *in vivo* activities of Mn(II) Schiff base coordination compounds for the *vitro* screening of manganese Schiff base coordination compounds, also as a result of available literature. The molecular docking entailed the use of Gaussian 03 created Schiff base ligand and HyperChem 8.0 created Mn(III) complex as ligands posed during interaction and binding with the amino acid group of the simulated and virtual breast cancer cell line (receptor).

11.1. Future Direction. Future direction will entail the review and comparative studies of anticancer activities of multinuclear manganese coordination compounds of Schiff base ligands and multidentate Schiff base ligands.

Data Availability

The data in the document and figures used to support the findings on this study are included within the article.

Conflicts of Interest

The author declares no conflicts of interest.

Acknowledgments

Ayodele Temidayo Odularu appreciates Govan Mbeki Research and Development Centre (GMRDC) for financial assistance.

References

[1] S. Sangram, "Maintaining good health should be the primary focus for everyone," 2021, https://www.brainyquote.com/quotes/sangram_singh_872637.

[2] M. Frezza, S. Hindo, D. Chen et al., "Novel metals and metal complexes as platforms for cancer therapy," *Current Pharmaceutical Design*, vol. 16, pp. 1813–1825, 2010.
[3] V. J. Yao, S. D'Angelo, K. S. Butler et al., "Ligand-targeted theranostic nanomedicines against cancer," *Journal of Controlled Release*, vol. 240, pp. 267–286, 2016.
[4] D. Cirri, F. Bartoli, A. Pratesi, E. Baglini, E. Barresi, and T. Marzo, "Strategies for the improvement of metal-based chemotherapeutic treatments," *Biomedicines*, vol. 9, no. 5, pp. 504–520, 2021.
[5] E. Boros, P. J. Dyson, and G. Gasser, "Classification of metal-based drugs according to their mechanisms of action," *Chem*, vol. 6, no. 1, pp. 41–60, 2020.
[6] P. Chellan and P. J. Sadler, "The elements of life and medicines," *Philosophical Transactions of the Royal Society A: Mathematical, Physical & Engineering Sciences*, vol. 373, no. 2037, pp. 20140182–20140256, 2015.
[7] U. Ndagi, N. Mhlongo, and M. Soliman, "Metal complexes in cancer therapy – an update from drug design perspective," *Drug Design, Development and Therapy*, vol. 11, no. 11, pp. 599–616, 2017.
[8] S. A. Cook, E. A. Hill, and A. S. Borovik, "Lessons from nature: abio-inspired approach to molecular design," *Biochemistry*, vol. 54, no. 27, pp. 4167–4180, 2015.
[9] M. P. Ngoepe and H. S. Clayton, "Metal complexes as DNA synthesis and/or repair inhibitors: anticancer and antimicrobial agents," *Pharmaceutical Fronts*, vol. 3, no. 4, pp. e164–e182, 2021.
[10] M. Poursharifi, M. T. Wlodarcyk, and A. J. Mieszawska, "Nano-based systems and biomacrmolecules as carriers for metallodrugs in anticancer therapy," *Inorga*, vol. 7, no. 1, pp. 1–19, 2019.
[11] D. L. Ma, C. Wu, S. S. Cheng, F. W. Lee, Q. B. Han, and C. H. Leung, "Development of natural product-conjugated metal complexes as cancer therapies," *International Journal of Molecular Sciences*, vol. 20, no. 2, pp. 341–415, 2019.
[12] A. T. Odularu, P. A. Ajibade, J. Z. Mbese, and O. O. Oyedeji, "Developments in platinum-group metals as dual antibacterial and anticancer agents," *Journal of Chemistry*, vol. 2019, Article ID 5459461, 18 pages, 2019.
[13] S. Thakurta and S. Khatua, "A drug design perspective of metal ions in medicine," *Archives of Chemistry and Chemical Engineering*, vol. 3, no. 1, 2021.
[14] K. J. Franz and N. Metzler-Nolte, "Introduction: metals in medicine," *Chemical Reviews*, vol. 119, no. 2, pp. 727–729, 2019.
[15] ES. Grassi, V. Vezzoli, I. Negri et al., "SP600125 has a remarkable anticancer potential against undifferentiated thyroid cancer through selective action on ROCK and p53 pathways," *Oncotarget*, vol. 6, no. 34, pp. 36383–36399, 2015.
[16] M. Delarmelina, R. D. Daltoé, M. F. Cerri et al., "Synthesis, antitumor activity and docking of 2, 3-(Substituted)-1, 4-naphthoquinone derivatives containing nitrogen, oxygen and sulfur," *Journal of the Brazilian Chemical Society*, vol. 26, pp. 1804–1816, 2015.
[17] M. Awatade, P. Ubale, A. Kamble et al., "Antitumor and antimicrobial potential of manganese(II), nickel(II) and copper(II) complexes of 4-methoxy benzohydrazide derived Schiff base ligand," *Letters in Applied NanoBioScience*, vol. 11, pp. 3249–3260, 2022.
[18] C. D'Sousa, J. H. A. Neto, D. R. B. BalizaIRS et al., "Novel piplartine-containing ruthenium complexes: synthesis, cell growth induction and ROS production on HCT116 cells," *Oncotarget*, vol. 8, no. 61, pp. 104367–104392, 2017.
[19] J. P. C. Coverdale, H. E. Bridgewater, J.-I. Song et al., "In vivo selectivity and localization of reactive oxygen species (ROS) induction by osmium anticancer complexes that circumvent platinum resistance," *Journal of Medicinal Chemistry*, vol. 61, no. 20, pp. 9246–9255, 2018.
[20] C. Sarma, P. K. Chaurasia, and S. L. Bharati, "Versatile catalytic applications of manganese(II, III) Schiff base complexes (Review)," *Russian Journal of General Chemistry*, vol. 89, no. 3, pp. 517–531, 2019.
[21] C. Sarma, S. L. Bharati, and P. K. Chaurasi, "Manganese Schiff base complexes and their biological catalytic applications," *Open Access Journal of Contraception*, vol. 4, no. 1, pp. 39–43, 2020.
[22] Z. Li, M. Niu, G. Chang, and C. Zhao, "Chiral manganese (IV) complexes derived from Schiff base ligands: synthesis, characterization, in vitro cytotoxicity and DNA/BSA interaction," *Journal of Photochemistry and Photobiology B: Biology*, vol. 153, pp. 473–482, 2015.
[23] E. B. Kurutas, "The importance of antioxidants which play the role in cellular response against oxidative/nitrosative stress: current state," *Nutrition Journal*, vol. 15, no. 1, pp. 71–22, 2016.
[24] X. Li, K. Zhao, W. J. Guo et al., "A novel manganese complex LMnAc selectively kills cancer cells by induction of ROS-triggered and mitochondrial-mediated cell death," *Science China Life Sciences*, vol. 57, no. 10, pp. 998–1010, 2014.
[25] A. W. Foster, D. Osman, and N. J. Robinson, "Metal preferences and metallation," *Journal of Biological Chemistry*, vol. 289, no. 41, pp. 28095–28103, 2014.
[26] J. D. Aguirre and V. C. Culotta, "Battles with iron: manganese in oxidative stress protection," *Journal of Biological Chemistry*, vol. 287, no. 17, pp. 13541–13548, 2012.
[27] Y. M. Garcia, A. Barwinska-Sendra, E. Tarrant, E. P. Skaar, K. J. Waldron, and T. E. Kehl-Fie, "A superoxide dismutase capable of functioning with iron or manganese promotes the resistance of Staphylococcus aureus to calprotectin and nutritional immunity," *PLoS Pathogens*, vol. 13, no. 1, pp. e1006125–19, 2017.
[28] C. Qiu-Yun, Z. Dong-Fang, H. Juan, G. Wen-Jie, and G. Jing, "Synthesis, anticancer activities, interaction with DNA and mitochondria of manganese complexes," *Journal of Inorganic Biochemistry*, vol. 104, no. 11, pp. 1141–1147, 2010.
[29] S. K. Ghosh, "Diversity in the family of manganese oxides at the nanoscale: from fundamentals to applications," *ACS Omega*, vol. 5, no. 40, pp. 25493–25504, 2020.
[30] S. L. O'Neal and W. Zheng, "Manganese toxicity upon overexposure: a decade in review," *Current Environmental Health Reports*, vol. 2, no. 3, pp. 315–328, 2015.
[31] C. J. Zhang, M. S. Valic, J. Chen, and G Zheng, "*In vivo* potential of manganese chelated porphysomes as MRI contrast agents," *STEM Fellowship Journal*, vol. 3, no. 1, pp. 47–53, 2017.
[32] S. J. S. Flora and V. Pachauri, "Chelation in metal intoxication," *International Journal of Environmental Research and Public Health*, vol. 7, no. 7, pp. 2745–2788, 2010.
[33] S. Pal, S. Mondal, R. Mukherjee, and J. Maity, "Removal of heavy metals from the body system by chelation therapy," *Journal of Nanomedicine & Nanotechnology*, vol. 2, no. 2, pp. 1–3, 2018.
[34] A. C. Martins Jr., P. Gubert, G. R. Villas Boas et al., "Manganese-induced neurodegenerative diseases and possible therapeutic approaches," *Expert Review of Neurotherapeutics*, vol. 20, no. 11, pp. 1109–1121, 2020.
[35] E. A. M. Khalil, W. H. Mahmoud, M. Eldessouky, and G. G. Mohamed, "Synthesis, spectral, thermal and biological

studies of some transition and inner transition Schiff base metal complexes," *Egyptian Journal of Chemistry*, vol. 64, 2021.

[36] A. T. Odularu, "Metal nanoparticles: thermal decomposition, biomedicinal applications to cancer treatment, and future perspectives," *Bioinorganic Chemistry and Applications*, vol. 2018, Article ID 9354708, 6 pages, 2018.

[37] Q. Al-anbaky, Z. Al-karakooly, S. P. Kilaparty et al., "Cytotoxicity of manganese (III) complex in human breast adenocarcinoma cell line is mediated by the generation of reactive oxygen species followed by mitochondrial damage," *International Journal of Toxicology*, vol. 35, no. 6, pp. 672–682, 2016.

[38] D. Milatovic and R. C. Gupta, "Manganese," *Veterinary Toxicology*, pp. 445–454, Academic Press, Cambridge, MA, USA, 3 edition, 2018.

[39] F. S. Al-Fartuise and S. N. Mohssan, "Essential trace elements and their vital roles in human body," *Indian Journal of Advances in Chemical Science*, vol. 5, no. 3, pp. 127–136, 2017.

[40] P. T. Bhattacharya, S. R. Misra, and M. Hussain, "Nutritional aspects of essential trace elements in oral health and disease: an extensive review," *Scientific*, vol. 2016, Article ID 5464373, 12 pages, 2016.

[41] K. D. Mjos and C. Orvig, "Metallodrugs in medicinal inorganic chemistry," *Chemical Reviews*, vol. 114, no. 8, pp. 4540–4563, 2014.

[42] A. Geersing, N. Ségaud, M. G. P. Van der Wijst, M. G. Rots, and G. Roelfes, "Importance of metal-ion exchange for the biological activity of coordination complexes of the biomimetic ligand N4Py," *Inorganic Chemistry*, vol. 57, no. 13, pp. 7748–7756, 2018.

[43] A. Kajal, S. Bala, S. Kamboj, N. Sharma, and V. Saini, "Schiff Bases: a versatile pharmacophore," *Journal of Catalysts*, vol. 2013, Article ID 893512, 14 pages, 2013.

[44] M. N. Uddin, S. S. Ahmed, and S. M. R. Alam, "REVIEW: biomedical applications of Schiff base metal complexes," *Journal of Coordination Chemistry*, vol. 73, no. 23, pp. 3109–3149, 2020.

[45] Z. Hussain, E. Yousif, A. Ahmed, and A. Altaie, "Synthesis and characterization of Schiff's bases of sulfamethoxazole," *Organic and Medicinal Chemistry Letters*, vol. 4, no. 1, pp. 1–4, 2014.

[46] D. A. Xavier and N. Srividhya, "Synthesis and study of Schiff base ligands," *IOSR Journal of Applied Chemistry*, vol. 7, no. 11, pp. 06–15, 2014.

[47] W. Qin, S. Long, M. Panunzio, and S. Biondi, "Schiff bases: a short survey on an evergreen chemistry tool," *Molecules*, vol. 18, no. 10, pp. 12264–12289, 2013.

[48] S. Slassi, A. Fix-Tailler, G. Larcher, A. Amine, and A. El-Ghayoury, "Imidazole and azo-based Schiff bases ligands as highly active antifungal and antioxidant components," *Heteroatom Chemistry*, vol. 2019, Article ID 6862170, 8 pages, 2019.

[49] S. Bhagat, N. Sharma, and T. S. Chundawat, "Synthesis of some salicylaldehyde-based Schiff bases in aqueous media," *Journal of Chemistry*, vol. 2013, pp. 1–4, Article ID 909217, 2013.

[50] N. Frankenberg, M. Schobert, J. Moser et al., "The biosynthesis of hemes, siroheme, vitamin B12 and linear tetrapyrroles in pseudomonads," in *Pseudomonas*, J. L. Ramos, Ed., Springer, Berlin, Germany, 2004.

[51] H. M. Abu-Soud, D. Maitra, J. Byun et al., "The reaction of HOCl and cyanocobalamin: corrin destruction and the liberation of cyanogen chloride," *Free Radical Biology and Medicine*, vol. 52, no. 3, pp. 616–625, 2012.

[52] M. O. Senge, N. N. Sergeeva, and K. J. Hale, "Classic highlights in porphyrin and porphyrinoid total synthesis and biosynthesis," *Chemical Society Reviews*, vol. 50, no. 7, pp. 4730–4789, 2021.

[53] M. Taniguchi and J. S. Lindsey, "Synthetic chlorins, possible surrogates for chlorophylls, prepared by derivatization of porphyrins," *Chemical Reviews*, vol. 117, no. 2, pp. 344–535, 2017.

[54] K. D. Borah and J. Bhuyan, "Magnesium porphyrins with relevance to chlorophylls," *Dalton Transactions*, vol. 46, no. 20, pp. 6497–6509, 2017.

[55] C. F. Zipp, J. P. Michael, M. A. Fernandes, and H. M. Marques, "The synthesis and characterization of several corroles," *South African Journal of Chemistry*, vol. 66, pp. 158–166, 2013.

[56] Â de Fátima, C. d P. Pereira, C. R. S. D. G. Olímpio, B. G. de Freitas Oliveira, L. L. Franco, and P. H. C. da Silva, "Schiff bases and their metal complexes as urease inhibitors - a brief review," *Journal of Advanced Research*, vol. 13, pp. 113–126, 2018.

[57] A. M. Abu-Dief and I. M. Mohamed, "A review on versatile applications of transition metal complexes incorporating Schiff bases," *Beni-Suef University Journal of Basic and Applied Sciences*, vol. 4, no. 2, pp. 119–133, 2015.

[58] Y. M. Ahmed, M. M. Omar, and G. G. Mohamed, "Synthesis, spectroscopic characterization, and thermal studies of novel Schiff base complexes: theoretical simulation studies on coronavirus (COVID-19) using molecular docking," *Journal of the Iranian Chemical Society*, vol. 19, no. 3, pp. 901–919, 2022.

[59] G. G. Mohamed, M. M. Omar, and Y. M. Ahmed, "Metal complexes of Tridentate Schiff base: synthesis, characterization, biological activity and molecular docking studies with COVID-19 protein receptor," *Zeitschrift für Anorganische und Allgemeine Chemie*, vol. 647, no. 23-24, pp. 2201–2218, 2021.

[60] M. S. More, P. G. Joshi, Y. K. Mishra, and P. K. Khanna, "Metal complexes driven from Schiff bases and semicarbazones for biomedical and allied applications: a review," *Materials Today Chemistry*, vol. 14, pp. 100195–100222, 2019.

[61] D. Lacopett, J. Ceramell, A. Catalano et al., *Applied Sciences*, vol. 11, pp. 1–20, 2021.

[62] T. Y. Fonkui, M. I. Ikhile, D. T. Ndinteh, and P. B. Njobeh, "Microbial activity of some heterocyclic Schiff bases and metal complexes: a review," *Tropical Journal of Pharmaceutical Research*, vol. 17, no. 12, pp. 2507–2518, 2019.

[63] S. Baluja and S. Chanda, "Synthesis, characterization and antibacterial screening of some Schiff bases derived from pyrazole and 4-amino antipyrine," *Rev Colomb Cienc Quím Farm*, vol. 45, no. 2, pp. 201–218, 2016.

[64] N. Muhammad and Z. Guo, "Metal-based anticancer chemotherapeutic agents," *Current Opinion in Chemical Biology*, vol. 19, no. 1, pp. 144–153, 2014.

[65] D. A. Rusanov, J. Zou, and M. V. Babak, "Biological properties of transition metal complexes with metformin and its analogues," *Pharmaceuticals*, vol. 15, no. 4, pp. 453–469, 2022.

[66] D. K. Awasthi, S. Gupta, and G. Awasthi, "Application of transition metal complex in medicine," *World Journal of Pharmaceutical and Medical Research*, vol. 5, no. 7, pp. 54–84, 2019.

[67] R. K. Sodhi and S. Paul, "Metal complexes in medicine: an overview and update from drug design perspective," *Cancer*

Therapy & Oncology International Journal, vol. 14, no. 2, p. 008, 2019.

[68] K. S. Egorova and V. P. Ananikov, "Toxicity of metal compounds: knowledge and myths," *Organometallics*, vol. 36, no. 21, pp. 4071–4090, 2017.

[69] M. Prejanò, M. E. Alberto, N. Russo, M. Toscano, and T. Marino, "The effects of the metal ion substitution into the active site of metalloenzymes: a theoretical insight on some selected cases," *Catalysts*, vol. 10, no. 9, pp. 1038–1128, 2020.

[70] J. P. T. Zaragoza and D. P. Goldberg, "Chapter 1: dioxygen binding and activation mediated by transition metal porphyrinoid complexes," in *Dioxygen-dependent Heme Enzymes*, pp. 1–36, RSC, London, UK, 2018.

[71] J. D. Kim, S. Senn, A. Harel, B. I. Jelen, and P. G. Falkowski, "Discovering the electronic circuit diagram of life: structural relationships among transition metal binding sites in oxidoreductases," *Philosophical Transactions of the Royal Society B*, vol. 368, no. 1622, pp. 20120257–20120259, 2013.

[72] J. M. Moulis, "Cellular dynamics of transition metal exchange on proteins: a challenge but a bonanza for coordination chemistry," *Biomolecules*, vol. 10, no. 11, pp. 1584–1626, 2020.

[73] J. Devi, M. Yadav, A. Kumar, and A. Kumar, "Synthesis, characterization, biological activity, and QSAR studies of transition metal complexes derived from piperonylamine Schiff bases," *Chemical Papers*, vol. 72, no. 10, pp. 2479–2502, 2018.

[74] A. Phaniendra, D. B. Jestadi, and L. Periyasamy, "Free radicals: properties, sources, targets, and their implication in various diseases," *Indian Journal of Clinical Biochemistry*, vol. 30, no. 1, pp. 11–26, 2015.

[75] G. L. Chang, Z. Li, M. J. Niu, and Su-Na Wang, "Studies on the manganese and copper complexes derived from chiral Schiff base: synthesis, structure, cytotoxicity and DNA/BSA interaction," *Journal of Coordination Chemistry*, vol. 72, no. 14, pp. 2422–2436, 2019.

[76] M. Haque, M. Z. Rahman, M. Pervin, M. H. Kabir, and M. S. Imran, "Biological screening of some ferrocene derivative metal complexes," *Pakistan Journal of Biological Sciences*, vol. 8, no. 12, pp. 1746–1750, 2005.

[77] I. R. Prihantono, R. Irfandi, and I. Raya, "Potential anticancer activity of Mn(II) complexes containing arginine dithiocarbamate ligand on MCF-7 breast cancer cell lines," *Annals of Medicine and Surgery*, vol. 60, pp. 396–402, 2020.

[78] M. Damercheli, D. Dayyani, M. Behzad, B. Mehravi, and M. Shafiee Ardestani, "New salen-type manganese(III) Schiff base complexes derived from meso-1, 2-Diphenyl-1, 2-ethylenediamine: in vitro anticancer activity, mechanism of action, and molecular docking studies," *Journal of Coordination Chemistry*, vol. 68, no. 9, pp. 1500–1513, 2015.

[79] H. Y. Qian and N. Sun, "Synthesis and crystal structures of manganese(III) complexes derived from bis-Schiff bases with antibacterial activity," *Transition Metal Chemistry*, vol. 44, no. 6, pp. 501–506, 2019.

[80] T. M. Seck, A. Sy, D. Lo et al., "Synthesis, spectroscopic studies and X-ray diffraction of heptacoordinated Mn(II) and Co(II) complexes with ligands derived from carbonohydrazide," *Open Journal of Inorganic Chemistry*, vol. 09, no. 4, pp. 35–52, 2019.

[81] M. R. Bermejo, R. Carballido, M. I. Fernández-García et al., "Synthesis, characterization, and catalytic studies of Mn(III)-Schiff base-dicyanamide complexes: checking the rhombicity effect in peroxidase studies," *Journal of Chemistry*, vol. 2017, Article ID 5465890, 10 pages, 2017.

[82] H. Keypour, N. Ansari, M. Mahmoudabadi et al., "Mn(III), Zn(II) and Pt(II) macroacyclic complexes: synthesis, X-ray structures, anticancer and antioxidant activities," *Inorganica Chimica Acta*, vol. 509, pp. 119705–119710, 2020.

[83] Z. Uyar, D. Erdener, I. Koyuncu, and Ü. Arslan, "Synthesis, characterization, and cytotoxic activities of a Schiff base ligand and its binuclear copper(II) and manganese(III) complexes," *Journal of the Turkish Chemical Society, Section A: Chemistry*, vol. 4, no. 3, pp. 963–980, 2017.

[84] R. A. Lal, A. Lemtur, S. Choudhury et al., "Synthesis and crystal structure of [Mn2(H2sal)2(hsal)2(H2O)4]. First example of the reductive synthesis of a binuclear manganese(I) salicylate complex," *Transition Metal Chemistry*, vol. 31, no. 4, pp. 423–428, 2006.

[85] J. Liu, W. Guo, J. Li et al., "Tumor-targeting novel manganese complex induces ROS-mediated apoptotic and autophagic cancer cell death," *International Journal of Molecular Medicine*, vol. 35, no. 3, pp. 607–616, 2015.

[86] K. Raval and T. Ganatra, "Basics, types and applications of molecular docking: a review," *IP International Journal of Comprehensive and Advanced Pharmacology*, vol. 7, no. 1, pp. 12–16, 2022.

[87] P. Müller, "Practical suggestions for better crystal structures," *Crystallography Reviews*, vol. 15, no. 1, pp. 57–83, 2009.

[88] S. Miriyala, I. Spasojevic, A. Tovmasyan et al., "Manganese superoxide dismutase, MnSOD and its mimics," *Biochimica et Biophysica Acta*, vol. 182, no. 5, pp. 794–814, 2012.

[89] Y. He, Q. Zhu, M. Chen et al., "The changing 50% inhibitory concentration (IC50) of cisplatin: a pilot study on the artifacts of the MTT assay and the precise measurement of density-dependent chemoresistance in ovarian cancer," *Oncotarget*, vol. 7, no. 43, pp. 70803–70821, 2016.

[90] P. Larsson, H. Engqvist, J. Biermann et al., "Optimization of cell viability assays to improve replicability and reproducibility of cancer drug sensitivity screens," *Scientific Reports*, vol. 10, pp. 5798–5812, 2020.

[91] N. S. Gwaram and P. Hassandarvish, "Synthesis, characterization and anticancer studies of some morpholine derived Schiff bases and their metal complexes," *Journal of Applied Pharmaceutical Science*, vol. 4, no. 10, pp. 075–080, 2014.

[92] A. S. Alturiqi, A. N. M. A. Alaghaz, R. A. Ammar, and M. E. Zayed, "Synthesis, spectral characterization, and thermal and cytotoxicity studies of Cr(III), Ru(III), Mn(II), Co(II), Ni(II), Cu(II), and Zn(II) complexes of Schiff base derived from 5-Hydroxymethylfuran-2-carbaldehyde," *Journal of Chemistry*, vol. 2018, Article ID 5816906, 17 pages, 2018.

[93] L. G. Ferreira, R. N. dos Santos, G. Oliva, and A. D. Andricopulo, "Molecular docking and structure-based drug design strategies," *Molecules*, vol. 20, no. 7, pp. 13384–13421, 2015.

[94] M. Damercheli, M. Mahdi, B. Mehravi, and M. Shafiee Ardestani, "Bioactive salen-type Schiff base transition metal complexes as possible anticancer agents," *Iranian Journal of Pharmaceutical Research*, vol. 18, no. 4, pp. 2055–2066, 2019.